University of Pardubice

Faculty of Chemical Technology

The application of pulsed laser deposition for the fabrication of thin films of materials for medicine

Bachelor's Thesis

2023 Maryia Muryna

Univerzita Pardubice
Fakulta chemicko-technologická
Akademický rok: 2021/2022

ZADÁNÍ BAKALÁŘSKÉ PRÁCE

(projektu, uměleckého díla, uměleckého výkonu)

Jméno a příjmení:	**Maryia Muryna**
Osobní číslo:	**C19394**
Studijní program:	**B0531A130012 Farmakochemie a medicinální materiály**
Téma práce:	**Využití pulzní laserové depozice pro přípravu tenkých vrstev medicinálních materiálů**
Téma práce anglicky:	**The application of pulsed laser deposition for the fabrication of thin films of materials for medicine**
Zadávající katedra:	**Ústav organické chemie a technologie**

Zásady pro vypracování

1. Seznamte se s literárně dostupnými informacemi o pulzní laserové depozici.
2. Proveďte literární rešerši o aplikacích pulzní laserové depozice pro přípravu tenkých vrstev medicinálních materiálů.
3. Vyhodnoťte a diskutujte nalezené poznatky s ohledem na budoucí potenciál.
4. Výsledky zpracujte formou závěrečné práce.

Rozsah pracovní zprávy:
Rozsah grafických prací:
Forma zpracování bakalářské práce: **tištěná**

Seznam doporučené literatury:

Veškerá dostupná odborná literatura.

Vedoucí bakalářské práce: **prof. Ing. Petr Němec, Ph.D.**
Katedra polygrafie a fotofyziky

Datum zadání bakalářské práce: **28. února 2022**
Termín odevzdání bakalářské práce: **1. července 2022**

L.S.

prof. Ing. Petr Kalenda, CSc. v.r.
děkan

prof. Ing. Miloš Sedlák, DrSc. v.r.
vedoucí katedry

DECLARATION

I declare:

The thesis entitled The application of pulsed laser deposition for the fabrication of thin films of materials for medicine is my own work. All literary sources and information that I used in the thesis are referenced in the bibliography.

I have been acquainted with the fact that my work is subject to the rights and obligations arising from Act No. 121/2000 Sb., On Copyright, on Rights Related to Copyright and on Amendments to Certain Acts (Copyright Act), as amended, especially with the fact that the University of Pardubice has the right to conclude a license agreement for the use of this thesis as a school work under Section 60, Subsection 1 of the Copyright Act, and that if this thesis is used by me or a license to use it is granted to another entity, the University of Pardubice is entitled to request a reasonable fee from me to cover the costs incurred for the creation of the work, depending on the circumstances up to their actual amount.

I acknowledge that in accordance with Section 47b of Act No. 111/1998 Sb., On Higher Education Institutions and on Amendments to Other Acts (Higher Education Act), as amended, and the Directive of the University of Pardubice No. 7/2019 Rules for Submission, Publication and Layout of Theses, as amended, the thesis will be published through the Digital Library of the University of Pardubice.

In Pardubice of the date 29.6.2023 Maryia Muryna b.o.h.

ACKNOWLEDGMENT

Here I would like to thank the supervisor of my thesis prof. Ing. Petr Němec, Ph.D. for his invaluable guidance and insightful advice during the process of working on this thesis. Last but not least I want to sincerely thank my family for providing me with the opportunity to pursue my education abroad, and my close friends for their unwavering support throughout my bachelor's studies.

ANOTACE

Tato bakalářská práce se zaměřuje na aplikaci pulzní laserové depozice pro výrobu tenkých vrstev, které se používají ke zvýšení kvality medicinálních materiálů. Poskytuje podrobný popis procesu PLD, jeho mechanismu a vybavení pro lepší pochopení toho, jak tato technika funguje. Kromě toho předvádí konkrétní studia, kde PLD technika byla úspěšně aplikována při depozici různých materiálů, což slouží jako příklady účinnosti dané techniky v oblasti medicinálních materiálů.

KLÍČOVÁ SLOVA

Pulzní laserová depozice, tenké vrstvy, medicinální materiály, biokompatibilita, implantáty.

ANNOTATION

This bachelor's thesis focuses on the application of pulsed laser deposition for the fabrication of thin films that are used to enhance the quality of medical materials. It provides a detailed description of the PLD process, its mechanism, and equipment for a better understanding of how this technique functions. Additionally, it showcases specific studies where PLD has been successfully applied to deposit various materials, serving as examples of its effectiveness in the field of medical materials.

KEYWORDS

Pulsed laser deposition, thin films, medical materials, biocompatibility, implants.

TABLE OF CONTENTS

LIST OF FIGURES 9

LIST OF ABBREVIATIONS 11

1 Introduction 13

2 Aim of the work 14

3 What Is PLD and How it works? 15

4 Pulsed laser deposition equipment 21

5 Use of PLD for the preparation of thin layers on medical materials 29

5.1 Calcium phosphate thin films 30

5.1.1 Hydroxyapatite thin films 31

5.1.1.1 Hydroxyapatite thin films on titanium substrate 32

5.1.1.2 Carbonate-substituted hydroxyapatite thin films on titanium substrate 34

5.1.1.3 Si-substituted hydroxyapatite thin films on titanium substrate 35

5.1.1.4 Ag-doped hydroxyapatite thin films on titanium substrates 36

5.1.1.5 Mg-doped hydroxyapatite thin films on porous titanium substrate 38

5.1.2 Calcium phosphate coatings on a polymeric ferroelectric substrate 39

5.1.3 Tricalcium phosphate thin films on calcium-doped magnesium alloys 41

5.1.4 Octacalcium phosphate thin films on titanium substrate 43

5.2 Bioactive glass and ceramic thin films 45

5.2.1 Bioactive glass thin films and coatings on titanium substrate 46

5.2.2 RKKP glass-ceramic thin films on titanium substrate 48

5.2.3 Cu-containing bioactive glass/eggshell membrane nanocomposites 49

5.3 Diamond-like Carbon thin films 51

5.3.1 Ag-incorporated Diamond-like Carbon thin films 54

5.3.2 Diamond-like Carbon coating of textile blood vessels 56

5.3.3 Si-incorporated Diamond-like Carbon thin films 57

6 Conclusion 59

7 Literature 60

LIST OF FIGURES

Figure 1: Schematic of the PLD process [1]. 15
Figure 2: Transmission electron microscope images of (b) nucleation, (c) growth, and (d) coalescence of Ag films on NaCl substrates (Modified by [24]). 19
Figure 3: Basic modes of thin film growth (a) layer by layer in the two-dimensional Frank-van der Merwe mode, (b) layer plus island in the Stranski-Krastanov mode, (c) island in the Volmer-Weber mode [25]. 20
Figure 4: Simplified schematic diagram illustrating the pulsed laser deposition set-up [2]. ... 22
Figure 5: The world's first large-area PLD tool developed in 1988 (Modified by [30]). 22
Figure 6: Schematic of a large-area PLD system utilizing laser rastering over large-diameter targets [1]. 23
Figure 7: Schematic of an active fluence compensation scheme for a large-area PLD system using large-diameter targets [22]. 24
Figure 8: Photographs of an Intelligent Window (Modified by [22,30]). 24
Figure 9: Typical spatial beam distributions of high pulse energy excimer (left) and Nd:YAG lasers (right) [31]. 26
Figure 10: Schematic of laser heater assembly showing the fiber-optic beam expander and pyrometer head (Modified by [22]). 27
Figure 11: Photograph of a set of Inconel substrate holders from a 5-inch PLD system [22]. 28
Figure 12: SEM micrograph of the cross-section of a PLD coating, showing a dense HA film [51]. 31
Figure 13: SEM micrographs revealing the surface morphology of the HA thin films by PLD on Ti-6Al-4V: (a and b) as-deposited HA; (c) HA coating annealed at 300 °C for 4 h [51]. ... 33
Figure 14: SEM micrographs of CHA films deposited on Ti substrates at 500 °C at (a) 1500 and (b) 10 000 magnification(left) and at 700 °C at (a) 1500 and (b) 10 000 magnification(right) [4]. 34
Figure 15: SEM images of different diameter sizes of TiO_2 nanotubes, (a) 30; (b) 50; (c) 70 and (d) 100 nm using a 200 nm scale bar [82]. 37
Figure 16: Comparative photographs of fungal populations (Candida albicans – a and b; Aspergilus niger – c and d), 24 h after incubation, on the heat-treated Ag-HA/nTiO_2/Ti films (b and d) and standard control samples (a and c) [81]. 37
Figure 17: Porous titanium-based implant used in the described study [86]. 38
Figure 18: SEM images of coating derived from PLD with HA target [55]. 40

Figure 19: SEM images of coatings derived from PLD with DCPA target [55].....40
Figure 20: SEM micrographs of TCP and Fe-TCP thin films obtained by PLD at RT and 300 °C. Scale bar A) 50 µm, B) 20 µm, C) 3 µm (upper images) and 5 µm (lower images) [109].42
Figure 21: OCP deposited on 316L stainless steel with NCD buffer layer: (a) 2D AFM image, (b) phase map [122].....44
Figure 22: SEM images of the cross section of CC films (A); DCPD films (B) formed after CC soaking in calcium nitrate solution for 168 h and final OCP films (C) formed after DCPD soaking in sodium acetate for 168 h [113].....44
Figure 23: SEM images (a) Titanium substrates; NbP-BG thin films deposited on Titanium substrates deposited (b) 50 mJ/cm^2 and (c) 100 mJ/cm^2 laser fluence, 10000× magnification. AFM inserts are at the same scale of figures. Modified by [140].....48
Figure 24: SEM micrographs of film deposited at 500 °C: (A) from the melt-processing RKKP target and (B) from the sol-gel RKKP target [33].....49
Figure 25: SEM analysis of the xCu-BG nanocoating on the surface of ESM films by the PLD technique. Outer ESM (a, b), 0Cu-BG/ESM (c, d), 2Cu-BG/ESM (e, f), 5Cu-BG/ESM (g, h). (a, c, e, and g) are low-magnification images, and (b, d, f, and h) are high-magnification images [147]. 51
Figure 26: Deposition system for coating of textile blood vessels: a photo of a vertical coating system, b scheme of the deposition system [156].....56
Figure 27: DLC-coated textile blood vessel of 7 mm diameter and 30 cm length (created in 0,25 Pa of argon, 20 J/cm^2) [156].....57

LIST OF ABBREVIATIONS

AFM	atomic force microscopy
Ag-DLC	silver-doped diamond-like carbon
Ag-HA	silver-doped hydroxyapatite
AR	anti-reflective
ArF	argon fluoride laser
BGs	bioactive glasses
BMMSs	bone marrow mesenchymal stem cells
CaP	calcium phosphate
CC	calcium carbonate
CHA	carbonate-substituted hydroxyapatite
Cu-BG	copper-containing bioactive glass
Cu-ESM	copper-containing bioactive eggshell membrane
DCPA	dicalcium phosphate anhydrous
DCPD	dicalcium phosphate dihydrate
DLC	diamond-like carbon
DRM	deposition rate monitor
ESM	eggshell membrane
Fe-TCP	iron-substituted tricalcium phosphate
HA	hydroxyapatite
HDLC	hydrogenated diamond-like carbon
IR	infrared
IW	intelligent window
k_B	boltzmann constant
KrF	krypton fluoride laser
Mg-HA	magnesium-doped hydroxyapatite
MSC	mesenchymal stem cells
NbP-BG	niobo-phosphate bioactive glass
NCD	nanocrystalline diamond
Nd:YAG	neodymium-doped yttrium aluminum garnet laser
OCP	octacalcium phosphate

PLD	pulsed laser deposition
PMMA	polymethylmethacrylate
PVDF	polyvinylidene fluoride
QCM	quartz crystal microbalance
R	deposition rate
R_0	equilibrium value
RBS	Rutherford backscattering spectrometry
RHEED	reflection high-energy electron diffraction
RKKP	glass-ceramic material named after Ravaglioli, Krajewski, Kirsch and Piancastelli
RT	room temperature
SBF	simulated body fluid
SEM	scanning electron microscopy
Si-DLC	silicon-infused diamond-like carbon
Si-HA	silicon-containing hydroxyapatite
TCP	tricalcium phosphate
VDF-TeFE	vinylidene fluoride-tetrafluoroethylene copolymer
VDF-TrFE	vinylidene fluoride copolymer with trifluoroethylene
XeCl	xenon fluoride laser
XPS	X-ray photoelectron spectroscopy
YBCO	yttrium barium copper oxide
$\Delta\mu$	supersaturation
μCT	X-ray microtomography
λ	wavelength
τ	pulse duration

1 Introduction

Advanced materials used in the field of medical materials are applied in order to increase the efficiency, security, and longevity of medical devices. Thin films have emerged as a promising approach for achieving these purposes, as they possess distinct qualities such as enhanced biocompatibility and customizable surface properties. Out of the numerous techniques available for depositing thin films, pulsed laser deposition has gained significant attention as a versatile and efficient method for producing thin films with precise control over their composition, thickness, and structure. PLD's capability to deposit films with precise atomic-scale accuracy allows for the production of coatings using different materials like metals, polymers, ceramics, and composites. These films exhibit exceptional adhesion, durability, and compatibility with a diverse range of substrates. Furthermore, the PLD process enables the incorporation of therapeutic agents such as antimicrobial substances, growth factors, and etc. Overall PLD is a technique with rich history and a promising future in the development of innovative medical materials with improved performance, biocompatibility, and patient outcomes.

2 Aim of the work

This thesis aims to investigate the application of PLD in the preparation of thin films for medical materials. The mechanism of pulsed laser deposition technique, while making accents on the most important parameters and its connection to the quality of obtained thin film, will be described. As well as equipment which is used and commercially available for PLD as the moment. Additionally, the thesis will explore specific case studies that highlight successful implementations of PLD in fabricating medical devices and implants, along with evaluations of their performance.

3 What Is PLD and How it works?

Pulsed laser deposition (PLD) is a popular technique used for growing thin films. This method became popular because of its simplicity [1,2] and the ability to deposit thin films with precise control over properties such as composition, thickness, and crystal structure [3,4]. By changing different characteristics of a process, such as a laser wavelength, background gas, target material and etc. It is possible to apply this technique for growing thin films of different kinds of materials [1,2]. Another factor that makes PLD highly intriguing and desirable is the possibility of stoichiometric transfer of target material towards the substrate in case of appropriate choice of ablation laser wavelength and absorbing target material [1,2,5]. PLD involves using a pulsed laser to focus on the material target that needs to be deposited. When the laser energy density is high enough, the material is vaporized or ablated by each laser pulse, resulting in the formation of a plasma plume. This plume is highly forward-directed and contains the ablated material that is ejected from the target. As a result, the ablation plume serves as the source of material flux for the growth of the film [1,2]. Although the design of PLD is simple, the actual process is surprisingly intricate and complicated [2]. The principle of PLD involves four complex physical processes [6,7]:

- interaction of a laser beam with a target
- ablation dynamics and plume formation
- ablated material deposition onto the substrate
- film growth

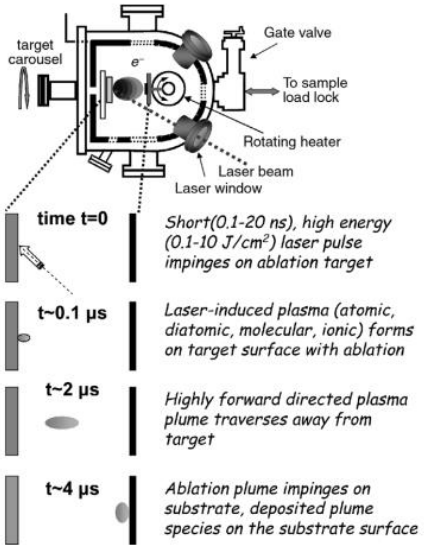

Figure 1: Schematic of the PLD process [1].

Interaction of a laser beam with a target

The PLD uses a high-intensity pulsed laser as a source of energy for evaporating a solid or liquid target material. When an incident laser beam hits the surface of the target, it is absorbed and energy is transferred to the electrons in a material [6]. When the material absorbs energy from the laser beam, it triggers oscillations of the electrons within the material. If the energy transferred by the laser beam to a single atom surpasses the atom's binding energy, the atom is expelled from the surface of the material [1,8].

Ablation dynamics and plume formation:

Pulsed laser deposition involves the ablation of a target material's surface through intense heating and material vaporization, which is primarily determined by the condition of the target surface and the bulk material's optical and thermal diffusion lengths. Due to the high pressure the vapor layer expands from the surface of the target and forms what is known as a plasma plume. The composition of the formed plume is similar in stoichiometry to that of the target material [6]. Plasma plume contains various species, such as ground- and excited-state neutral atoms, electrons, and ions, which expand out from the target [9,10]. These species then are deposited on the substrate and form the film [8]. The resulting vapor plume, consisting of partially ionized material, expands primarily in a forward direction due to pressure gradients. As the vapor plume moves away from the target surface, its thermal energy is converted into the directed kinetic energy of the atoms and ions. It is fundamental to control the composition of the plasma plume generated by the laser since this has a significant impact on the quality of the resulting film. If the plume contains macroscopic particles and liquid droplets, it can result in low-quality deposited films [11].

The ablation mechanism and, in turn, the quality of the resulting film depends on the key growth parameters, which can be broadly divided into three categories: (i) laser properties, such as pulse duration, wavelength, and fluence, (ii) the type and pressure of the background gas, and (iii) the substrate type and temperature [12,13].

(i) laser properties

The laser wavelength that is employed for ablation must be taken into account. In order to effectively ablate the target material, it is necessary to stimulate the ablated volume into a non-equilibrium state at temperatures significantly higher than those required for evaporation [1].

The laser's wavelength primarily determines how deeply it penetrates into the target material. To prevent the production of numerous particles on the film surface, the laser must be absorbed mainly in a thin layer close to the target surface, without causing subsurface boiling [14]. For instance, common laser wavelengths PLD users select are ArF (193 nm, or 6,42 eV), KrF (248 nm, or 4,99 eV), XeCl (308 nm, or 4,03 eV), and Nd:YAG (1064 nm, or 1.16 eV) [8]. Types of lasers used in the PLD technique will be discussed in the Chapter 4.

Laser fluence is another important laser quality that has a great effect on film growth. If the laser has low fluence or if the target material doesn't absorb the laser's wavelength well, the laser will only heat the target. This can cause the target to evaporate due to the heat. When the laser fluence (energy density) increases, it will reach a point where the energy absorbed by the target is more than the energy required for evaporation. This point is called the ablation threshold and depends on the material's absorption coefficient, which is also related to the laser's wavelength. At even higher fluences, the ablated material will absorb the laser, creating a plasma on the target surface [1].

(ii) Background gas

PLD can occur either in a vacuum or with the addition of a dilute background gas to control the composition of the film [10]. When PLD is carried out in a vacuum, the plume doesn't expand only in one direction, but also in the opposite direction because of the high plasma density [15,16]. The particles released in the plume spread out and interact with each other, which makes them quickly lose their energy. Also, the plume in a vacuum is only visible near the target [10]. Selecting the appropriate type and pressure of the background gas is fundamental for producing a thin film with the desired composition, thickness, and crystalline structure [15,17]. This is an important factor in controlling the kinetic energies of the deposited particles on the substrate, controlling the addition of other elements such as O from O_2, C from CH_4, or N from NH_3 for example, and regulating the thickness of the film [2]. Usually, the thin films are created in the presence of a reactive background gas, like oxygen which is used to make oxide films, nitrogen which is used for nitride films, or hydrogen [2,18]. Alternatively, noble background gases like helium, neon, and argon are commonly used as background gases in PLD. These gases are relatively inert and can provide a low-pressure environment for the ablated plume to expand and reach the substrate [2,15,19]. They can also help to cool down the

substrate and the deposited film, which is important for preventing unwanted reactions or thermal damage to the substrate [15,19].

(iii) the substrate type and temperature

The substrate material used in PLD depends on the application of the deposited film [1,8]. In general, the substrate should be chemically stable and have a crystal structure similar to that of the deposited material to promote epitaxial growth [8]. Selecting a substrate with the highest structural and chemical match with the thin film material significantly contributes to superior surface morphology and lower defect density of the thin film [20]. The substrate can be made of materials like silicon, quartz, sapphire, or other materials, depending on the properties of the deposited film required. For example in Group III nitride film growth sapphire is the most widely used [12].

The substrate temperature is one of the PLD technique's process parameters that directly influences the mobility rate, re-evaporation, nucleation, growth, and crystallization of deposited species on the substrate surface, which in turn impacts the microstructure and thin film's characteristics [21]. Typically in thin-film growth, the substrate temperature is chosen to be 50-75% of the melting temperature of the film. The substrate temperature is generally in the range of 200-1000°C, depending on the target material and the desired film properties [12]. For instance, to deposit high-quality thin films of oxide materials like YBCO, the substrate temperature should be maintained at around 700°C to ensure the proper stoichiometry and crystallinity of the film [22]. It is worth mentioning that if the amorphous thin film is being deposited, the substrate is not heated. They are deposited at low temperatures, which leads to reduced mobility of the adatoms on the substrate, preventing crystalline structure formation [23].

The Evaporation of the Ablated Materials onto the Substrate

There are three phases in the mechanisms of interaction between the incident plume flux and the substrate: (1) atoms being sputtered by an intense incident plume from the substrate's surface and (2) a collision region (thermalized region) being formed between the incident plume and the sputtered atoms. The area of collision acts as a source for particle condensation, which triggers the last stage of the process, that is, (3)the growth of the film [6]. How the ablated

species is evaporated onto the substrate greatly affects the thin film's quality. The various laser characteristics, such as the laser energy, pulse repetition rate, and number of pulses, may have an impact on this. These laser characteristics may have an impact on the energy of the species that are ejected and land on the substrate [18]. In particular, very high plume densities could cause harm to the substrate [6].

Film growth

Thin film growth consists of nucleation, growth, and coalescence (Figure 2) [8,24]:

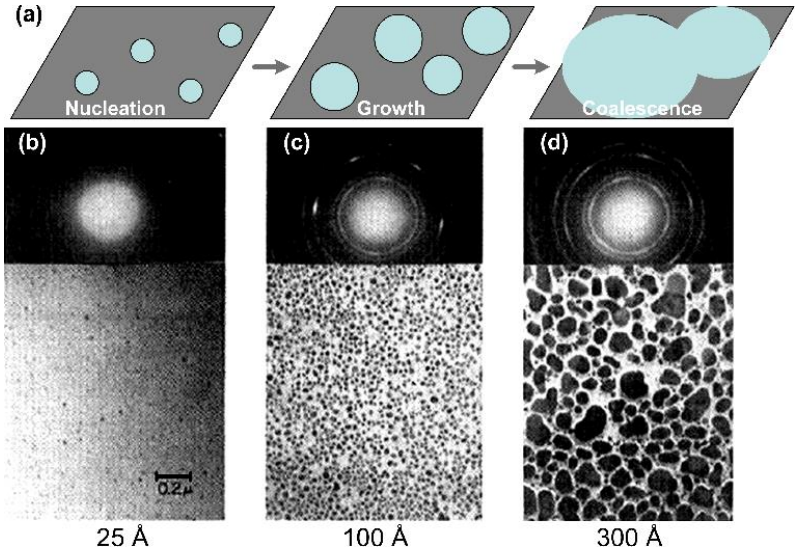

Figure 2: Transmission electron microscope images of (b) nucleation, (c) growth, and (d) coalescence of Ag films on NaCl substrates (Modified by [24]).

The film undergoes a transition from the plasma (plume) phase to a crystalline (solid) phase during the nucleation and growth stage on the substrate surface. The nucleation and growth of crystalline thin film are dependent on various factors such as laser energy, pulse repetition rate, density and degree of ionization of the ablated material, substrate temperature, physicochemical properties of the substrate, and background pressure. However, the substrate temperature (T) and the supersaturation (Δμ) between the plasma and solid phase during crystallization are the two significant thermodynamic parameters involved in the growth mechanism. These two parameters are related by an equation [6,11]:

$$\Delta\mu = k_B T \, ln \frac{R}{R_0} \tag{1}$$

where k_B is the Boltzmann constant, R is the actual deposition rate, and R_0 is its equilibrium value at temperature T [11]. Equation (1) indicates that the degree of supersaturation increases proportionally with the temperature of the substrate. A low level of supersaturation results in the formation of large nuclei, which leads to the development of scattered patches (or islands) of the film on the substrate's surface [6]. For all phase transitions, the formation of thin films is characterized by the formation of nuclei and their growth. Depending on the interaction energies of substrate atoms and film atoms [24] any of the common modes of thin film growth can occur [8,25] (Figure 3):

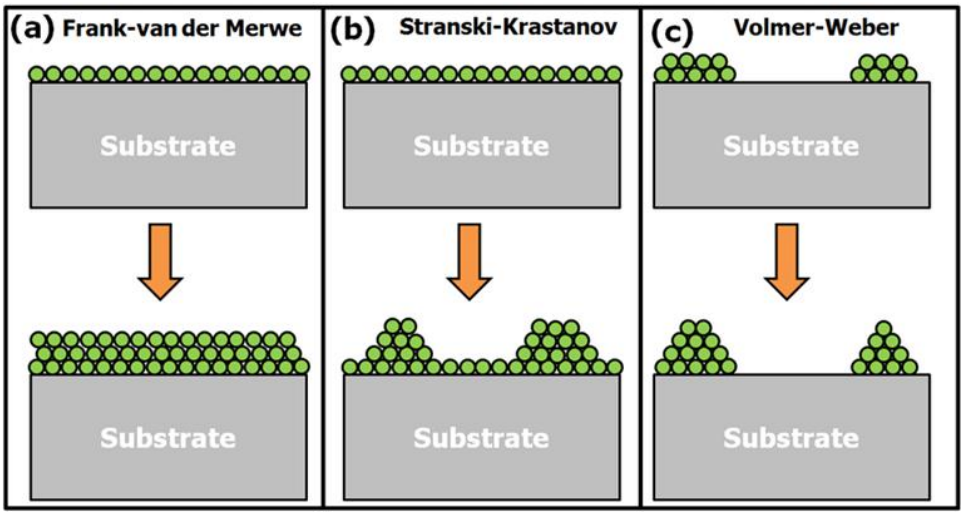

Figure 3: Basic modes of thin film growth (a) layer by layer in the two-dimensional Frank-van der Merwe mode, (b) layer plus island in the Stranski-Krastanov mode, (c) island in the Volmer-Weber mode [25].

2D layer-by-layer, or Frank–van der Merwe, growth happens when the energy that binds adatoms (atoms on the surface) to each other is the same as, or weaker than, the energy that binds them to the substrate (the surface they are growing on) [26,27]. This particular mode is utilized to carry out the epitaxial synthesis of two-dimensional (2D) materials such as silicene, germanene, or stanene, as well as multi-layered structures containing quantum wells [28].

In *3D, or Volmer-Weber, island growth*, stable clusters form into 3D islands that combine to create a complete film. The shape of the formed islands can be different [8]. This type of growth happens when the adatoms stick more tightly to each other than to the substrate, which is common for metal films on insulators or dirty substrates (surfaces that don't interact strongly with the film and have high energy at the interface) [26,27]. Metals being deposited on gas-metal compounds such as SiO_2, NaCl, and TiO_2 is a classic example of island growth. These

gas-metal compounds have comparatively low surface energies with saturated surface bonds, whereas metal surface energies are considerably higher [27].

The third growth mode, called *Stranski-Krastanow*, is a mixture of the first two. Initially, one or more 2D layers of a heterostructure are formed. However, it becomes harder to add more layers, and 3D islands form instead. This process is also called islanding or strain-induced roughening. The switch from 2D to 3D happens when it takes more energy to add another layer than to create 3D islands, which can partly relieve the strain through expansion [26,27].

In PLD, deposition and growth occur at different times, allowing to measure kinetic parameters for various growth conditions. This is achieved by monitoring the decay of the adatom density between the deposition pulses [27]. Reflection high-energy electron diffraction (RHEED) is commonly employed to examine film surface processes and mechanisms during growth. It relies on the diffraction of electrons by surface atoms and offers valuable insights into the periodic arrangement of these atoms [27,29], the surface quality of the substrate, the growth mode of the film and the number of atomic layers deposited when following a layer-by-layer growth mode [8].

4 Pulsed laser deposition equipment

PLD equipment typically includes a laser, a target material, a vacuum chamber, and a substrate holder (Figure 4). PLD equipment can be designed to deposit a wide range of materials, including metals, oxides, nitrides, and semiconductors. The equipment can also be designed to deposit films on a variety of substrate materials, including silicon, glass, and polymers [22].

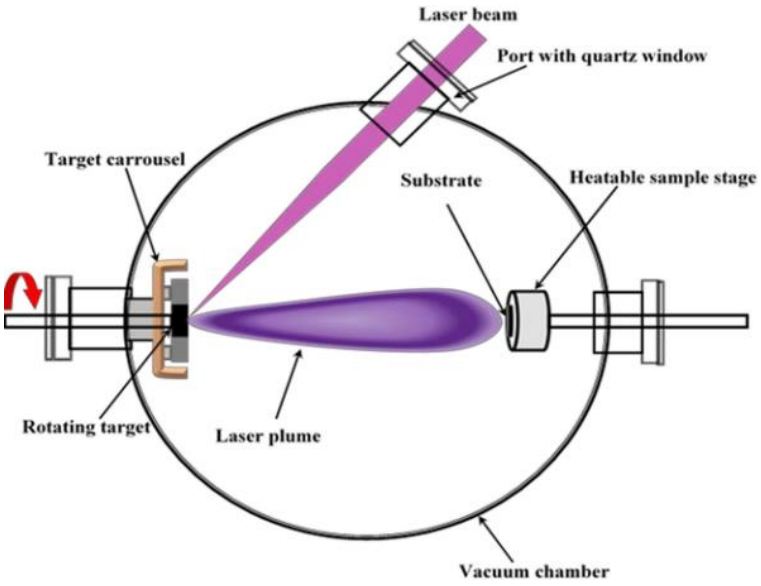

Figure 4: Simplified schematic diagram illustrating the pulsed laser deposition set-up [2].

With the rediscovery of PLD in the late 1980s [1] the materials science community was filled with an immense sense of enthusiasm, which led to significant in-house development of PLD tools. These tools were specifically designed for small areas, usually around 1 cm^2 in size [30]. As one scales up the PLD process, various obstacles needed to be overcome, such as laser power and beam stability, proper design of the optical components, robust substrate heaters, large target size and motion, and deposition rate monitoring [22].

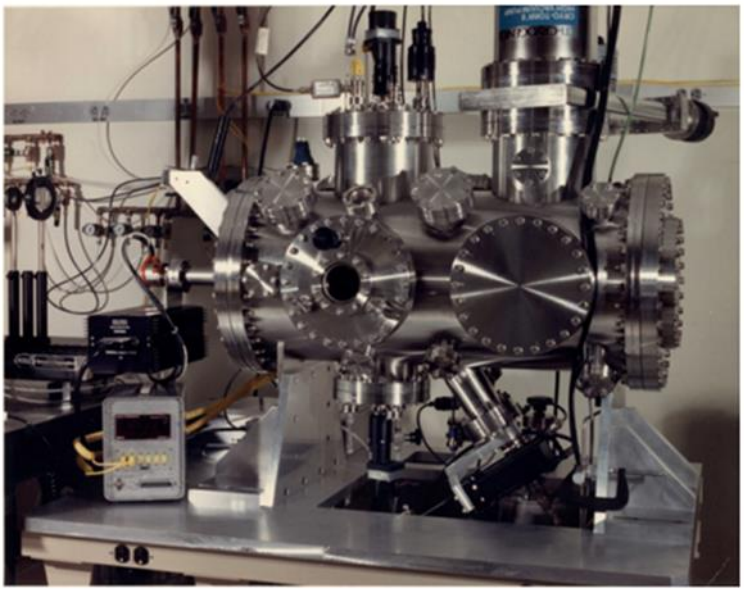

Figure 5: The world's first large-area PLD tool developed in 1988 (Modified by [30]).

Since 1992, laser beam rastering has been used to scale up to larger substrate sizes (Figure 6). A mirror mounted on a kinematic mount is used to raster the laser across a rotating ablation target, while the substrate is rotated offset from the target. The raster pattern depends

on various parameters, including laser beam size, shape, orientation, target-to-substrate distance, background gas pressure, and substrate temperature. Typically, the target diameter is larger than the substrate, and the raster scan rate is slow compared to substrate or target rotation speeds [22].

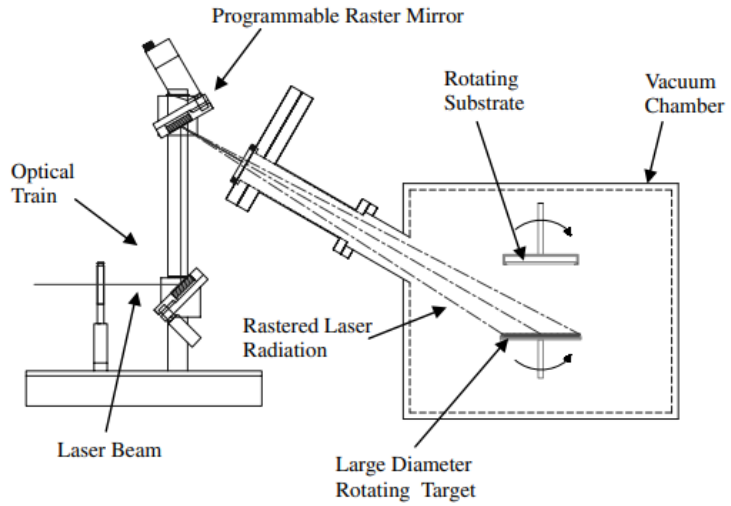

Figure 6: Schematic of a large-area PLD system utilizing laser rastering over large-diameter targets [1].

As the size of the substrate increases, it becomes increasingly important to use higher laser power to achieve practical average film growth rates. When it comes to producing films with useful deposition rates, lasers with higher repetition rates and slightly lower pulse energy are more suitable than those with higher energy per pulse and lower repetition rates. Excimer lasers are the most cost-effective option for large-scale commercial implementation of the PLD process. This is because they can reliably deliver average powers ranging from 6 W up to 300 W at 248 nm (KrF) or 308 nm (XeCl) [22].

Ensuring constant fluence at the target surface is a crucial challenge that must be adequately addressed when implementing large-area PLD with large-diameter targets and laser beam scanning. To overcome this issue, modern optical beam delivery systems incorporate active beam compensation with large-diameter targets. To maintain a consistent laser beam path, the positioning of the focusing lens is synchronized with the raster mirror. This means that when the focusing lens is positioned at point *a*, the raster mirror ensures that the laser beam is focused at point *a* on the target. The same applies to position *c* and any other position along the target surface (Figure 7) [22].

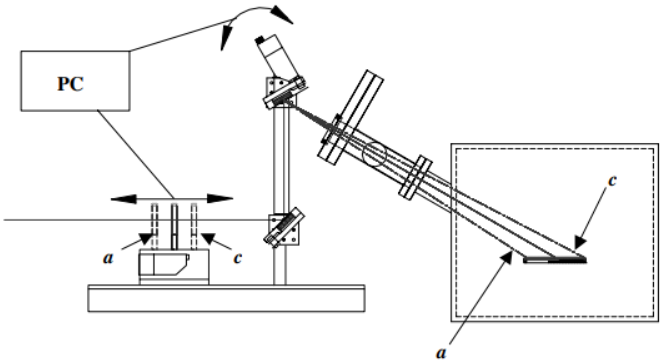

Figure 7: Schematic of an active fluence compensation scheme for a large-area PLD system using large-diameter targets [22].

Intelligent Windows

The Intelligent Window (IW) (Figure 8) was developed in 1992 to resolve the issue of maintaining a clean laser beam path for prolonged periods [3]. The window in the IW is made up of two vacuum flanges that hold a large, see-through, ultraviolet (UV) fused silica disk. This disk is located between an anti-reflective (AR) coated optic, which lets the laser beam enter the deposition chamber, and a molybdenum aperture on the other side. The fused silica disk catches the ablated material that travels back toward the AR-coated optic. The coated section of the disk is only as large as the aperture, which reduces the laser energy by a certain amount (usually around 10%). To ensure even coating, the window can be rotated to expose a new section of the disk to the laser and backscattered material. Once the entire disk is coated, it can be replaced with a new one [22].

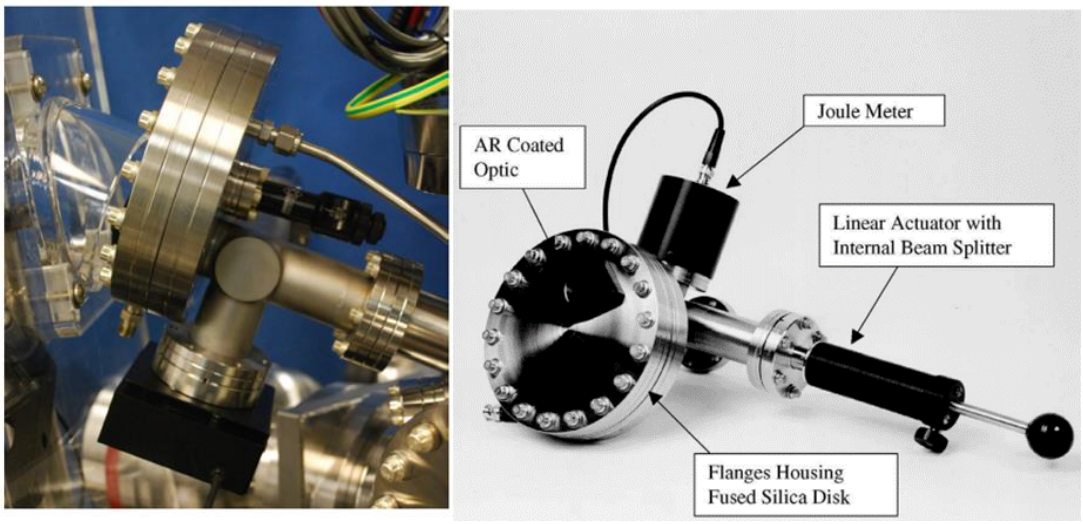

Figure 8: Photographs of an Intelligent Window (Modified by [22,30]).

The IW has a useful feature that allows for the measurement of energy that travels through the entire optical system. A beam splitter can be inserted into the beam path using a linear actuator, which reflects the beam back out of the chamber to a UV detector. This allows for the precise monitoring and adjustment of energy that passes through the system, including the laser, lens, mirrors, and window, before or during deposition. Additionally, the IW's disk rotation and energy measurement features can be automated if needed [22].

Lasers used for ablation

The laser used in PLD is a critical component that provides the energy necessary to generate the plasma plume and deposit high-quality thin films. There are several types of lasers that can be used for PLD, but the most common are excimer lasers, gas lasers, and Nd:YAG lasers [8,22]. Inert gases are used in gas lasers, which primarily emit visible light. On the other hand, excimer lasers employ a combination of reactive gases such as fluorine and chlorine with inert gases such as argon, krypton, or xenon. Upon electrical stimulation of excimer lasers, dimers are formed, and this results in the emission [19] of short pulses of ultraviolet light, typically at 193 nm or 248 nm wavelengths. These lasers (exomers) are commonly used for depositing thin films of oxides and nitrides, as well as other materials. Ultraviolet (UV) laser radiation is, in general, much better absorbed by most materials, so short wavelengths are preferable in many applications with picosecond lasers [22].

Excimer lasers offer significant advantages over Nd:YAG lasers in thin film manufacturing due to their superior ablation characteristics and better energy stability. These advantages are particularly evident in terms of optical properties. Conversely, Nd:YAG lasers are associated with a number of major drawbacks in the context of pulsed laser deposition. These include an inherently inappropriate gaussian beam profile, which does not provide a flat-top profile. Additionally, temperature-induced polarization and thermal lensing effects can create a donut-shaped beam profile and lateral distortions, further compromising the suitability of Nd:YAG lasers for PLD (Figure 9) [2,31].

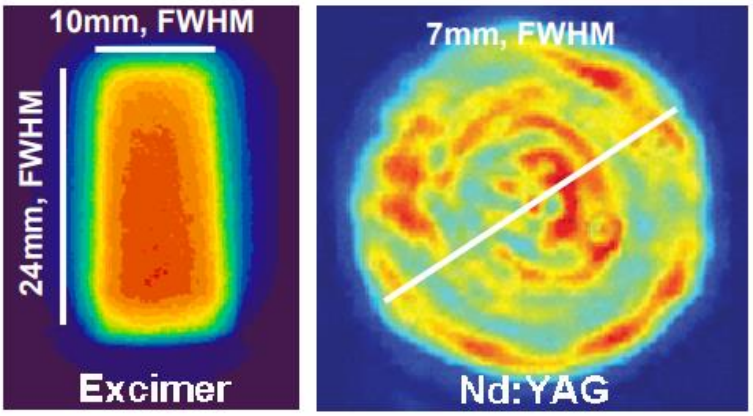

Figure 9: Typical spatial beam distributions of high pulse energy excimer (left) and Nd:YAG lasers (right) [31].

Other types of lasers that can be used for PLD include dye lasers, Ti:sapphire lasers, and copper vapor lasers. The choice of laser depends on the specific material being deposited, the desired film properties, and the available equipment [22].

Substrate Heaters

In PLD growth processes, the substrate temperature is an essential factor to consider. However, when the substrate is rotating, it can be challenging to monitor its temperature using a thermocouple. Measuring the temperature of materials like silicon is relatively easy using most pyrometers at temperatures above 600°C. But for transparent substrates like sapphire or $LaAlO_3$, measuring their temperature using pyrometers is difficult at wavelengths where measurements are typically taken. Pyrometers will usually measure the temperature of any structure behind the transparent substrate. A pyrometer that can measure the temperature of IR transparent substrates would be highly beneficial for the PLD process [22].

Substrate heaters are an important component of any PLD system, as they help to heat up the sample being studied. There are three different types of heating systems used in PLD: resistive-type heaters, infrared (IR) lamp heaters, and laser heaters [22].

Resistive-type heaters are the most basic and inexpensive type of heater. They usually consist of a metal block with a heating element inside, basic low-cost resistive heaters usually utilize an Inconel sheath heating element brazed to an Inconel block, which can heat samples up to 950°C. However, when using resistive heaters, the sample must be bonded to the heater block using a silver or platinum paste to ensure good thermal conductivity. This method works well for small samples but can become problematic for larger samples [22].

Other types of heaters, such as IR and boroelectric heaters, are also available. However, these heaters should not be used with oxygen and should not be raised above 750°C, as this can cause damage to the system [22].

Laser heaters are another option, which can heat small samples to very high temperatures. Figure 10 shows a schematic of the laser heater principle. Laser heaters work by using a laser to heat up the substrate, which is placed near the heater block. Laser heating is good for small sample sizes and provides fast ramp times, high substrate temperatures, and the ability to work with most process gases. However, it is not practical for substrates larger than 2.5 cm in diameter [22].

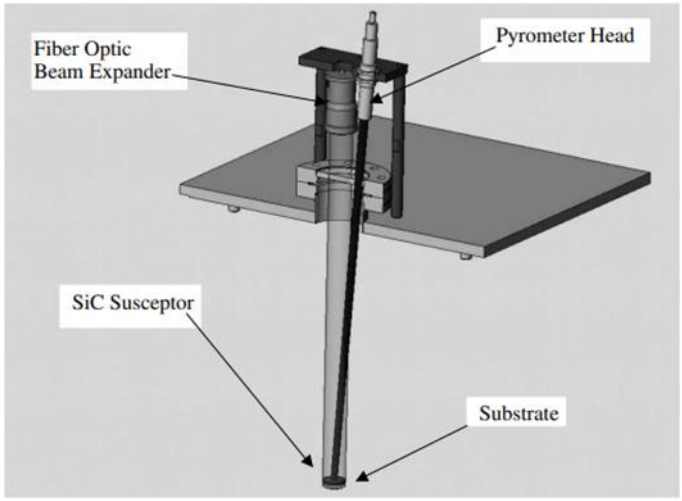

Figure 10: Schematic of laser heater assembly showing the fiber-optic beam expander and pyrometer head (Modified by [22]).

IR lamp heaters are effective for heating samples in PLD systems without using silver paste. Lamps emit IR and visible light, with peak blackbody emission at 1200 K or higher. Water-cooled housings minimize the heat load on internal components and chamber walls. Substrates are placed in Inconel rings at the edges, and reflective coatings or shields minimize heat losses. Figure 11 shows a range of substrate holders for a 5-inch PLD system [22].

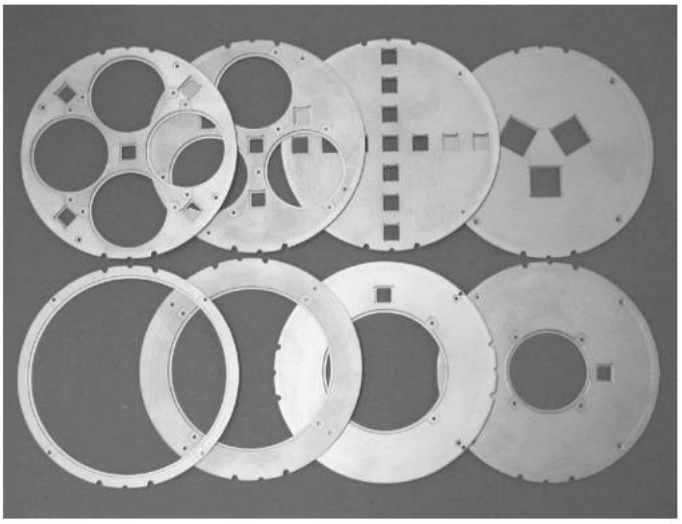

Figure 11: Photograph of a set of Inconel substrate holders from a 5-inch PLD system [22].

Overall, the type of heater chosen depends on the particular application and budget of the end user [22].

Target Size

Selecting the appropriate target size is important when designing a PLD system. Small 1-inch-diameter targets work well for small substrates, but larger targets are necessary for achieving consistent results and uniform films as the substrate size increases. This is important not only from run to run but also within a single run [22].

When using large substrate heaters, heating the target can become an issue if the target diameter is also large. Most commercial PLD systems prevent this problem by placing a large water-cooled plate directly above the target's surface. This plate has a slot that allows the laser beam to reach the target and for the plume to expand toward the substrate. The radiation from the substrate will heat the center of the target more than the edges, leading to uneven thermal expansion and causing the large-diameter target to crack. Despite this, cracked targets are frequently used in large-area PLD systems without any significant impact on the quality of the resulting films [22].

Deposition Rate Monitors

Deposition Rate Monitors (DRMs) are used in PLD to measure and control the deposition rate of the material onto the substrate during the process to achieve uniform films

with reproducible results. Typically, a quartz crystal is used as the DRM, which vibrates at a known frequency. As the material is deposited onto the crystal, its mass increases, causing a shift in the crystal's vibration frequency. This shift in frequency is then used to calculate the deposition rate. Regrettably, a Quartz Crystal Microbalance (QCM) is not suitable for large-area PLD processing. A rate monitor based on atomic absorption was developed, but it experienced various problems. Ellipsometry can be used for monitoring deposition rates, but it's limited to specific materials. Reflection high-energy electron diffraction is another technique used for monitoring film growth rates, but it's not practical for large-area systems when deposition pressures are high. Typically, for large-area films of a particular thickness, the deposition process relies on the total power incident on the target, time, and previous experience with the target and material. However, using an in situ fluence monitor like the Intelligent Window can help achieve more precise thickness measurements. By monitoring the energy before it hits the target, the Intelligent Window can improve the accuracy of film thickness measurements, leading to better quality films [22].

5 Use of PLD for the preparation of thin layers on medical materials

In the context of medical materials, PLD is particularly attractive due to its ability to produce thin films of bioactive, biocompatible, and highly adherent materials [32,33]. These properties are important for applications such as implants and prosthetics, where the material needs to integrate with the body's tissues without causing any adverse reactions or immune responses [32,34]. PLD is also a versatile method that can be used to deposit a wide range of materials, including ceramics [33], metals [35,36], and polymers [32,37]. This makes it useful for producing medical materials with specific mechanical, chemical, and biological properties to suit a variety of clinical needs. Overall, the use of pulsed laser deposition for producing medical materials offers many advantages, including ease of implementation, efficiency, and the ability to create uniform and complex structures. As such, it is a promising technique for the development of new and improved medical materials in the future [32]. This section of the thesis aims, to discuss the fabrication of diverse biomaterials utilizing the pulsed laser deposition technique while highlighting their inherent qualities and potential applications.

5.1 Calcium phosphate thin films

Calcium phosphate (CaP) is an example of an orthophosphate. There are many different types of CaP compounds, including hydroxyapatite, fluorapatite, oxyapatite, octacalcium phosphate, etc. The molar Ca/P ratio and solubility are the main factors that set them apart from one another. The atomic ratio of Ca to P in pure compounds ranges from 0.5 to 2 [32]. The stability, reactivity, degradability, and mechanical properties of calcium phosphates are largely influenced by the Ca/P ratios [38]. As the Ca/P ratio decreases, materials tend to become more acidic and water-soluble [32]. The Ca/P ratio of films obtained is dependent on the specific deposition control parameters applied during the PLD process [39,40]. For example, calcium phosphates with a Ca/P ratio of 1.67 are known as hydroxyapatite (HA) [41,42]. HA is one of the most popular and well-studied calcium phosphates, Chapter 5.1.1 will be entirely devoted to this material. Tricalcium phosphate (TCP), which has a Ca/P ratio of 1.5 is another example of calcium phosphate. TCP has been the subject of extensive research for its applications as a drug-delivery agent and as an injectable cement used to fill bone defects [41].

When it comes to medical devices, the surface of the implant is the first point of contact with the host body. Therefore, surface modifications are significant in improving the biocompatibility and osteoconductive properties of these devices [43]. One way to improve the compatibility of implant surfaces with bone is by coating an artificial material with a thin layer of calcium phosphate. This method has proven effective in enhancing the biocompatibility and osteoconductivity of the base material [44]. Calcium phosphate makes up a significant portion of bone (about 60% by weight) and is the primary component of tooth enamel (around 90%) [42]. CaP, promote the formation of bone tissue and form a direct bond with the surrounding bone tissue [45]. The primary process involved in the bioactivity of CaP is the partial dissolution of the material, which leads to the release of ionic products inside the body [46,47]. Depositing calcium phosphate films on medical implants allows for the combination of the superior mechanical strength of metallic implants with the excellent bioactivity provided by the surface layers of calcium phosphates [48].

The deposition of CaP thin films by PLD was first described by Cotell [49]. When PLD is used to prepare biocompatible CaP thin films, depositions are mostly performed using a UV KrF excimer laser [50-53], Nd:YaG [54,55], or ArF excimer laser [48,56]. The pulsed laser deposition method provides flexibility in controlling the morphology, phase, crystallinity, and chemical composition of the resulting thin films. These characteristics play a big role in the bio-

resorption or dissolution process, which directly affects the osseointegration of the calcium phosphates films [39,57]. The significance of surface characteristics in determining the effectiveness of an implant is widely acknowledged [58]. Regardless of the initial surface roughness, coatings produced using the PLD technique tend to exhibit a rough texture (Figure 12) [51].

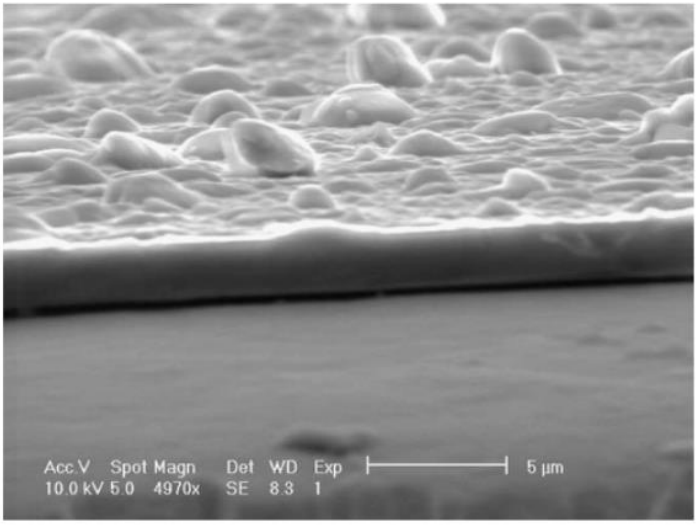

Figure 12: SEM micrograph of the cross-section of a PLD coating, showing a dense HA film [51].

The upcoming chapters will be dedicated to exploring different types of calcium phosphate materials, their applications, and the synthesis of coatings using the pulsed laser deposition technique.

5.1.1 Hydroxyapatite thin films

Hydroxyapatite is one of the most significant calcium phosphate compounds with regard to bioactivity and biocompatibility. Hydroxyapatite, with the chemical formula $Ca_{10}(PO_4)_6(OH)_2$, is a crystalline hydrated calcium phosphate. Its crystal structure and chemical composition are the same as the minerals found in bones and teeth [59]. Of all calcium phosphates, HA is the most stable and least soluble in aqueous media [32]. Due to its chemical and structural resemblance to human hard tissues (50% mass, 70% volume), and the fact that it is the main constituent of bones and teeth [60], it is one of the most well-known and extensively studied biocompatible materials and is utilized as an implantable ceramic [61]. HA does have some drawbacks, though. For instance, HA ceramics have poor mechanical qualities, are exceedingly fragile, and break readily in bulk, especially in damp settings [62]. Because of this,

HA cannot be employed in orthopedic devices that need to sustain heavy loads for the duration of their predicted lives. To get around this problem, HA can be coated on metallic implants or other non-load-bearing surfaces as a very thin layer [63]. PLD has significant advantages when used to produce bioceramics based on HA. It can create HA films that are pure, crystalline, and have the correct composition. Additionally, it allows for control over the shape, structure, crystallization, and chemical properties of the obtained films [32]. Chapter 5.1.1 provide examples illustrating the production and application of thin films made from hydroxyapatite.

5.1.1.1 Hydroxyapatite thin films on titanium substrate

Orthopedic implant materials are now primarily made of titanium and alloys based on titanium [64]. But it is known that Ti-based alloys are classified as bioinert materials, as they do not stimulate bone growth on their surfaces [65]. Titanium in its unmodified state is susceptible to bacterial infections, which can cause inflammation and eventually lead to implant failure. It is widely acknowledged that preventing the initial bacterial adhesion is essential to impede the formation of biofilms [66,67]. To improve the qualities of titanium and its alloys it is possible to modify titanium surface with various coatings. This would result in an implant with higher wear resistance since the coatings would provide biocompatibility, oxidation protection, increased corrosion resistance, and hardness [4]. Coatings made of hydroxyapatite have been used to solve the issue of bioinertness because they have been shown to boost the bioactivity of implant surfaces [65].

Dinda and his colleagues conducted an investigation where hydroxyapatite was deposited on a titanium substrate. The study employed commercially accessible sintered HA-dense discs as target materials, while rolled sheets of Ti-6Al-4V were utilized as substrates. The deposition was performed in an ultrahigh vacuum deposition chamber using a KrF excimer laser source with laser wavelength set at 248 nm and laser fluence set at 3 J/cm^2, at ambient temperatures with the use of oxygen as a background gas [51].

Regardless of laser deposition parameters (laser fluence, chamber pressure, gas environment), using pulsed laser deposition at room temperature resulted in the formation of amorphous thin films, according to the research [51]. However, for medical implants, it is important for the hydroxyapatite films to be crystalline as amorphous HA films dissolve slowly in bodily fluids [68]. Achieving crystalline structure from amorphous films is possible through

annealing these films. In the case, of Dinda's work desired crystalline structure was achieved at 300 °C after 4 hours of annealing [51].

SEM and AFM analysis of the PLD-produced HA thin films demonstrated their dense nature, along with uniformly distributed droplets on the surface of the deposited films (Figure 13). These surface droplets are significant as they enhance the bioactivity of the implants by increasing the total surface area, thereby promoting cell growth and proliferation, which is improving implant performance [51].

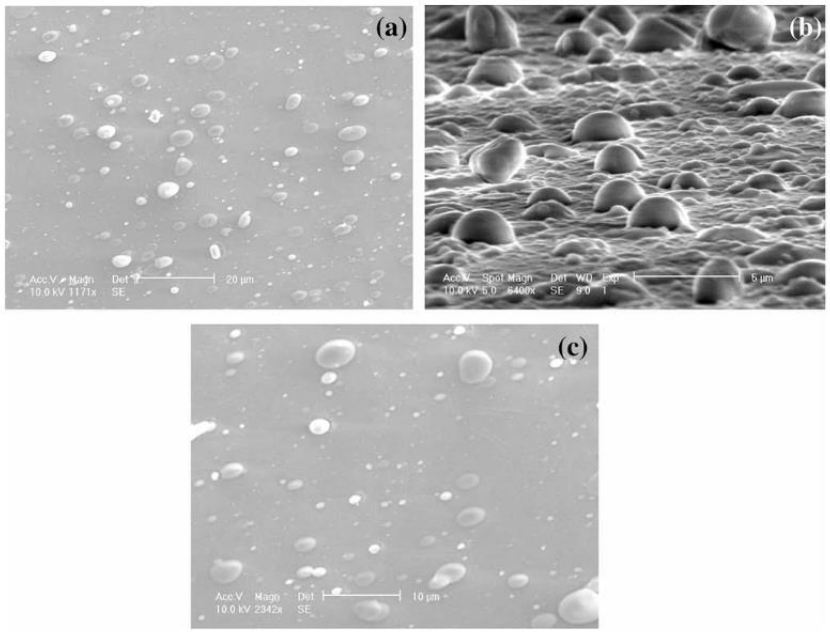

Figure 13: SEM micrographs revealing the surface morphology of the HA thin films by PLD on Ti-6Al-4V: (a and b) as deposited HA; (c) HA coating annealed at 300 °C for 4 h [51].

Dinda's findings indicate that when comparing crystalline hydroxyapatite films to amorphous HA films, the former demonstrate superior mechanical strength, hardness, and Young's modulus. These crystalline films also display excellent adhesion to Ti-6Al-4V substrates even at lower annealing temperatures. Furthermore, the crystalline HA coatings exhibit enhanced resistance to dissolution when exposed to simulated body fluid (SBF). Obtained results of described research showed that a combination of PLD and annealing is a suitable method for the preparation of crystalline HA films on titanium substrate for medical applications [51].

5.1.1.2 Carbonate-substituted hydroxyapatite thin films on titanium substrate

Julietta Rau and her colleagues conducted an investigation where carbonate-substituted hydroxyapatite was deposited on titanium substrates. Carbonate-substituted hydroxyapatite (CHA) was synthesized according to reaction (1) between calcium oxide, ammonium hydrogen phosphate, and ammonium carbonate [4]:

$$10CaO + 6(NH_4)_2HPO_4 + (NH_4)_2CO_3 + 4H_2O \rightarrow Ca_{10}(PO_4)_6\text{-}yCO_3(OH)_2\text{-}z + 14NH_3.H_2O;\ 3y + z = 2 \qquad (1)$$

Films were deposited on the treated Ti substrates at different substrate temperatures (namely: 30, 200, 400, 500, 700, and 750 °C) in a high-vacuum PLD chamber. Depositions were performed by focusing a pulsed KrF excimer laser (λ = 248 nm, τ = 17 ns) on the sintered CHA rotating target. The total deposition time was 15 min [4].

After analyzing the obtained samples, it was found that in the temperature range of 30-500 °C, about 9 µm thick amorphous films were formed, characterized by large domains (Figure 14) (500-600 nm of average height, 60 nm of average roughness). At higher deposition temperatures (700 °C), 4 µm thick CHA films with a more compact and finely granulated surface morphology (Figure 12) (15-30 nm of average grain height, 20 nm of average roughness) were obtained. At this temperature, the achieved films were crystalline and medium-textured [4].

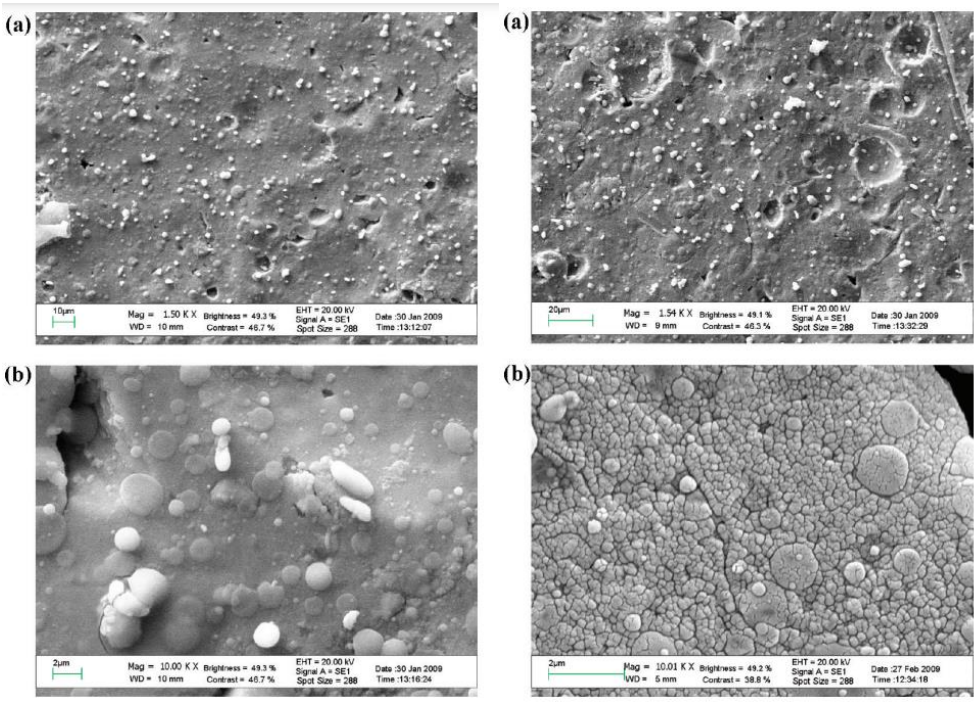

Figure 14: SEM micrographs of CHA films deposited on Ti substrates at 500 °C at (a) 1500 and (b) 10 000 magnification(left) and at 700 °C at (a) 1500 and (b) 10 000 magnification(right) [4].

From systematic analysis it can be seen that PLD deposition carried out at 700 °C enables the production of CHA films with all the essential properties needed for biomedical implant application. These films also exhibited good crystallinity, a medium degree of roughness, and increased hardness [4].

5.1.1.3 Si-substituted hydroxyapatite thin films on titanium substrate

Human bone tissues contain silicon, a benign trace element whose ion form, silicate, has a direct impact on bone growth and development [69]. Hydroxyapatite, changed with the inclusion of small concentrations of silicon has shown an improvement in osteoblast proliferation and bone extracellular matrix production [70]. Additionally, it is hypothesized that Si substitution can boost solubility, provide a more electronegative surface, and thin out the microstructure, changing the implant surface into a more biologically comparable apatite [71].

The pulsed laser deposition approach is one of the many methods for creating Si-HA films that are now accessible, and it shows great promise for producing coatings of excellent quality. Due to the employment of laser light in a vacuum, this method has several special advantages such as the lack of contamination [72,73].

Solla and co-workers have done two studies comparing the composition transfer in pulsed laser deposition of Si-HA thin films, using Si of different sources: metallic Si, synthetic SiO_2, and diatomaceous earth, a biological source of SiO_2 [72,73].

The initial study on incorporating Si into HA structure involved creating Si-HA film coatings on Ti substrates using laser ablation of commercial HA and metallic Si powder mixtures. The proportion of Si in the ablation targets (ranging from 0-10 at.%) determined the composition of the coatings. The ablation process was conducted using an ArF excimer laser and the films were deposited in a water vapor atmosphere at 460°C. XPS (X-ray photoelectron spectroscopy) experiments gave information about how Si atoms were bonded and how much Si was transferred to the coating from the ablation target [72].

The second study investigated the use of synthetic SiO_2 and diatomaceous earth as sources of Si for producing silicon-substituted hydroxyapatite coatings on pure HA targets through laser ablation. It followed the same direction as previous research. Results showed that both sources were suitable for incorporating Si into the film and controlling the desired quantity of Si. However, the diatomaceous earth series showed a higher concentration of ionic traces as

found by RBS (Rutherford Backscattering Spectrometry), which makes it a better candidate for producing Si-HA thin films that mimics the composition of biological bone more efficiently [73].

Overall both studies concluded that utilizing PLD in a water vapor atmosphere is a viable technique for producing Si-HA thin films on Ti substrates [72,73].

5.1.1.4 Ag-doped hydroxyapatite thin films on titanium substrates

In Chapter 5.1.1.1, titanium and its alloys were mentioned as highly suitable biomaterials. However, despite their benefits, the use of these materials does not always guarantee successful outcomes. It was mentioned earlier that unmodified titanium, in particular, is susceptible to bacterial infections, which can cause inflammation and ultimately lead to implant failure [67]. As mentioned above, using HA coating could help improve the osteoconductivity and biocompatibility of titanium implants [65]. Recent studies have emphasized that using a silver-doped HA thin films could improve antimicrobial and osteogenic properties [74,75]. According to research, silver has been identified as one of the most effective agents for controlling bacterial adhesion and preventing biofilm formation. Silver has been recognized for its broad antibacterial spectrum and oligodynamic bactericidal activity in various biomedical applications since ancient times, and has been the subject of extensive study due to its potent antimicrobial properties [76,77]. Furthermore, silver has been found to be effective against a broad spectrum of drug-resistant microorganisms and has been approved for use in various medical devices for more than two decades [78]. It is important to highlight that an excessive amount of Ag can be harmful and result in severe illness if it's not accurately incorporated into the hydroxyapatite structure [79]. Because of that, it is essential to optimize the amount of silver in the HA lattice, so it is possible to obtain optimal antimicrobial activity in the samples without causing any harm [80].

In the manuscript done by Erakovic and team, HA and Ag-HA thin films were synthesized by pulsed laser deposition on pure Ti and porous Ti, which is Ti modified with 100 nm diameter TiO_2 nanotubes substrates (Figure 15). The deposition of the HA and Ag-HA thin films was conducted by ablation of respective targets with a KrF excimer laser source ($\lambda = 248$ nm, $\tau \leq 25$ ns). Applied laser fluence was set at 4.5 J/cm^2 (with a corresponding laser energy of 435 mJ). For the deposition of each film, 15000 subsequent laser pulses have been applied [81].

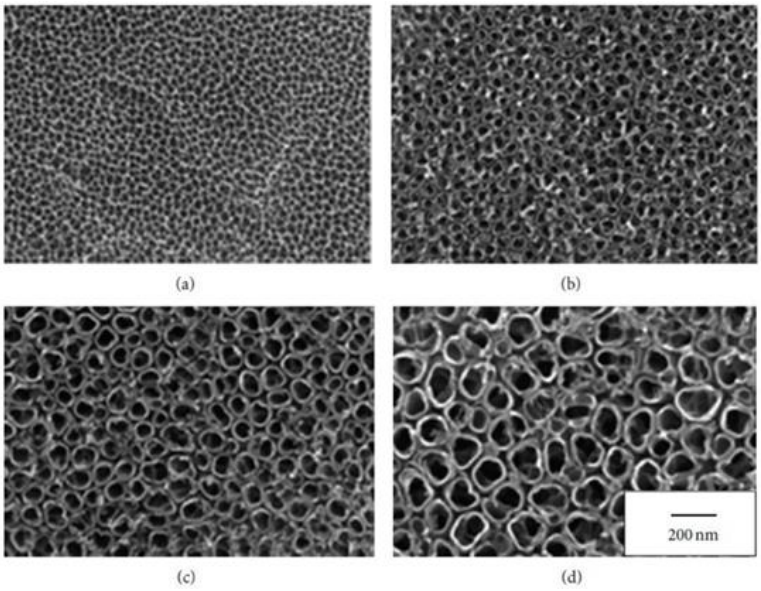

Figure 15: SEM images of different diameter sizes of TiO_2 nanotubes, (a) 30; (b) 50; (c) 70 and (d) 100 nm using a 200 nm scale bar [82].

According to the findings of physical-chemical investigations and cytotoxicity testing, heat-treated Ag-HA thin films deposited on Ti modified by TiO_2 nanotubes substrates have a radical antifungal action against the two strains, causing the reduction of colonies by 99.73% in the case of Aspergillus niger and complete extermination in case of Candida albicans colonies (Figure 16) [81].

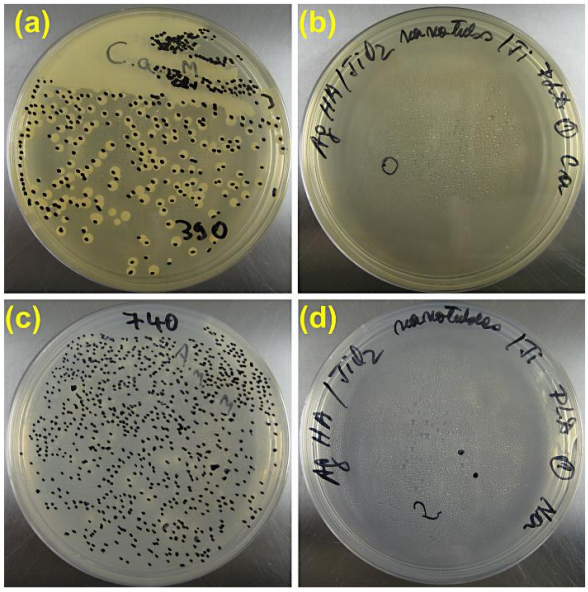

Figure 16: Comparative photographs of fungal populations (Candida albicans – a and b; Aspergilus niger – c and d), 24 h after incubation, on the heat-treated Ag-HA/nTiO_2/Ti films (b and d) and standard control samples (a and c) [81].

In summary, the study found that depositing Ag-HA thin films on Ti modified with TiO_2 nanotubes substrates using PLD, effectively creates barriers that prevent adherence and contamination by pathogenic fungi [81].

5.1.1.5 Mg-doped hydroxyapatite thin films on porous titanium substrate

Another alternative for enhancing titanium implant proliferation and osseointegration is magnesium. Studies have shown that Mg^{2+} has a stimulating effect on proliferation when incorporated into HA [83]. When assessed in vivo, Mg-HA granulate was found to be as effective, if not superior to traditional HA as a bone substitute. Specifically, Mg-HA displayed superior osteoconductivity over time and higher material resorption compared to stoichiometric HA [84].

In a study done by Mróz and the team, they deposited Mg-HA on porous titanium alloy implants (Figure 17) using pulsed laser deposition [85]. Titanium porous alloys were mentioned in a previous chapter. They offer several advantages over solid scaffolds. These advantages include a larger surface area for the bone to attach, the possibility of bone growing into the holes or spaces, which improves the connection between the implant and bone, and a lower stiffness that reduces the difference in stiffness between the implant and bone, lowering the risk of bone loss caused by stress [86].

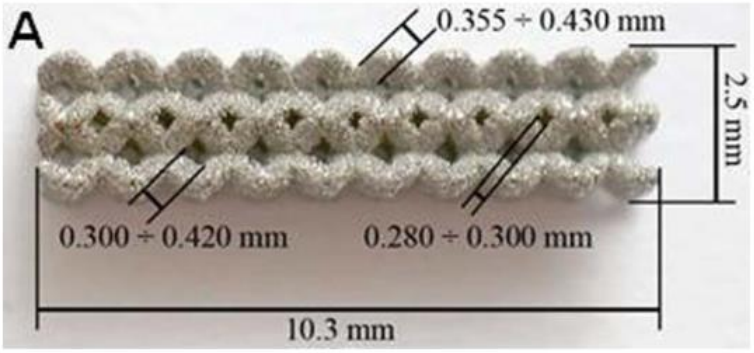

Figure 17: Porous titanium-based implant used in the described study [86].

The PLD process was performed in a water vapor atmosphere with an average temperature of implant 410°C. The deposition of thin film was conducted by ablation of the respective target with a yttrium-doped fiber laser with the laser fluence set at 4.7 J/cm². For the deposition of a film, 2200 subsequent laser pulses have been applied [85].

In vivo studies of the received implant with magnesium-doped hydroxyapatite thin film coating have been done. This studies involved the placement of implants in the femoral condyles of rabbit hind paws. According to μCT (X-ray microtomography) studies, implants coated with Mg-HA showed a clear superiority over uncoated implants in terms of bone volume. Furthermore, the studies also revealed that newly formed bone was able to penetrate through the mesh and reach the center of the implanted material [85].

5.1.2 Calcium phosphate coatings on a polymeric ferroelectric substrate

Fluoropolymers are widely used in medical implants due to their advantageous properties [87]. These include excellent chemical resistance, strong mechanical characteristics, heat resistance, thermal stability, and biological inertness [88]. Some specific fluoropolymers, such as polyvinylidene fluoride (PVDF), vinylidene fluoride with tetrafluoroethylene copolymer (VDF-TeFE), and vinylidene fluoride copolymer with trifluoroethylene (VDF-TrFE), possess piezoelectric and ferroelectric properties [89]. The ferroelectric nature of PVDF and its copolymers allows for the active manipulation of biological cell populations on their surfaces. Studies have shown that an increase in the ferroelectric β phase promotes the differentiation of MSC (mesenchymal stem cells) into osteoblasts [90,91]. leading to accelerated bone tissue regeneration [92]. One significant drawback of PVDF and its copolymers in implant applications is their limited ability to integrate effectively with tissues, primarily due to their low surface-free energy [93,94]. To overcome this limitation and facilitate bone tissue regeneration on fluoropolymer surfaces, calcium phosphate coatings are commonly applied [95]. Pulsed laser deposition emerges as a promising technique for creating calcium phosphate coatings on ferroelectric polymer materials, as it addresses two crucial requirements: achieving the desired roughness of the CaP coating and preserving the crystal structure of the polymer while retaining its ferroelectric properties [55].

In a work conducted by Bolbasov and co-workers two types of targets were utilized: hydroxyapatite and Dicalcium Phosphate Anhydrous ($CaHPO_4$, DCPA) in the form of pressed powders [55]. HA is a widely used compound in calcium phosphates, its properties were described in Chapter 5.1.1. DCPA is notable for its bioactivity and has practical applications in dental cements and restorative materials [96]. In vitro evaluations revealed that DCPA facilitated active osteoclast resorption and stimulated higher expression levels of osteogenic genes in bone marrow cells [97,98]. Additionally, it was reported that DCPA fillers accelerated

bone regeneration and achieved a better balance between substitute resorption and new bone formation compared to HA [99].

Bolbasov and co-workers used as a substrate copolymer VDF-TeFE. For ablation, the fundamental harmonic of a repetitively pulsed solid-state Nd:YAG laser was applied with a wavelength of 1064 nm and a maximum laser fluence of 5 J/cm^2. The whole process was carried out in vacuum. The research findings obtained through SEM and AFM techniques revealed that under the chosen conditions of coating formation, both types of sputtering targets resulted in a complex and multiscale roughness structure on the coated surface (Figure 18, Figure 19). This suggests that the rough surface of the coatings formed in this study can enhance the attachment of osteoblasts and promote bone formation in vivo [55].

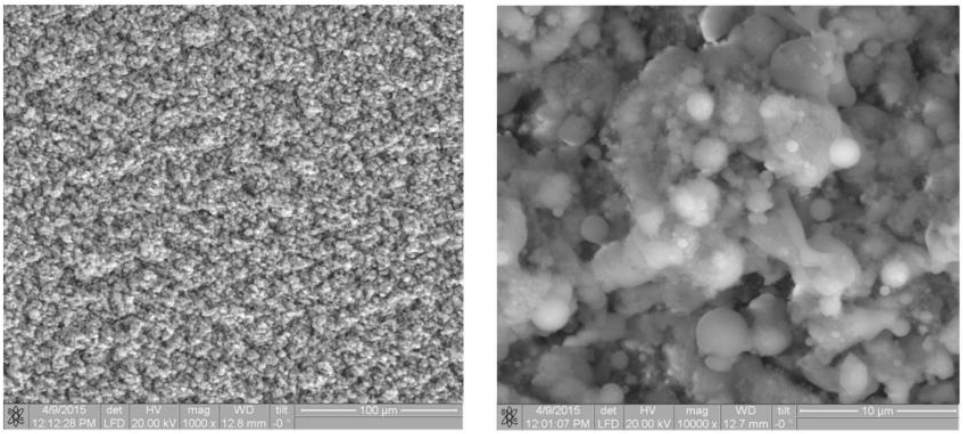

Figure 18: SEM images of coating derived from PLD with HA target [55].

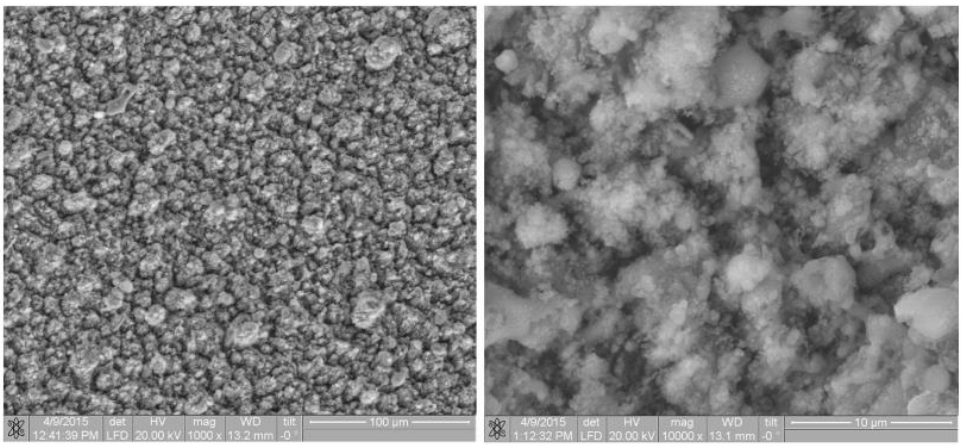

Figure 19: SEM images of coatings derived from PLD with DCPA target [55].

The described study showed that PLD is an applicable technique for the deposition of HA and DCPA on a polymeric ferroelectric substrate, as obtained coatings preserved the properties of the ferroelectric film without altering the substrate's crystal structure. Furthermore

the rough surface topography and high Ca and P content in the PLD-formed HA and DPCA coatings contributed to their cell-rich surface [55].

5.1.3 Tricalcium phosphate thin films on calcium-doped magnesium alloys

The use of magnesium and its alloys as degradable materials for implants has sparked considerable interest [100-102]. These alloys hold promise for orthopedic and cardiovascular implants, as they eliminate the need for additional removal surgeries [103]. A notable advantage is the release of Mg^{2+} ions upon degradation, which contribute to various cellular reactions, regulating metabolism and protein synthesis [104]. However, a significant drawback of magnesium-based alloys is their limited corrosion resistance [105,106]. To address this problem, a possible solution is to apply biocompatible and biofunctional coatings on magnesium-based alloys. This can effectively enhance their corrosion resistance and improve their suitability as implant materials [107,108]. Applying CaP thin films is a way to improve the compatibility of implant surfaces with bone. In Chapter 5.1 it was mentioned that a thin layer of CaP material has the ability to improve the biocompatibility and osteoconductivity of the underlying material [44]. Tricalcium phosphate is a favorable choice for coating inorganic implant surfaces due to its outstanding biocompatibility and degradability. It is frequently utilized as a bone repair material in various applications [109].

In a work implemented by Antoniac and co-workers, TCP thin films were applied on biodegradable Mg-Ca alloys using the PLD technique [109]. The inclusion of Ca in the alloy system is advantageous as it contributes to a low density (1,55 g/cm^3), similar to that of bone [110]. Additionally, magnesium plays a big role in facilitating calcium incorporation into the bone [111], which can be beneficial for bone healing by enabling the co-release of Mg and Ca ions [110]. The aim of Antoniac's work was to enhance the corrosion resistance and reduce the degradation rate of the alloys. In addition to pure TCP coatings, they also explored the deposition of iron-substituted tricalcium phosphates (Fe-TCP). Fe was chosen as a doping element because it is one of the trace elements in living tissue that participates in oxidation-reduction reactions in energy metabolism. In general, doping TCP with the necessary trace elements may impart it with extra-functional properties [109]. Recent studies have investigated iron-substituted tricalcium phosphate, which has shown promising characteristics such as low cytotoxicity, high cell viability, and antibacterial activity [108,112].

As an irradiation source, a Nd:YAG laser with four harmonics was used. Laser fluence was adjusted on 2 J/cm^2. Four films were deposited, two thin films from the TCP target and two thin films from the Fe-TCP targets, both from the substrate heated at 300 °C and substrate kept at RT. The thicknesses of deposited coatings were approximately 2 μm ± 5%. SEM analysis showed that pure TCP thin films had uniform dispersion of particles, while Fe-TCP layers had a dense structure with nanoparticle accumulation. TCP samples obtained at room temperature exhibited rod-like particle morphology, with particle size reduction at higher temperatures. Incorporating Fe transformed rods into spheres, resulting in a mixture of spheres and rods in Fe-TCP thin films (Figure 20B), with particle size reduction observed at 300 °C [109].

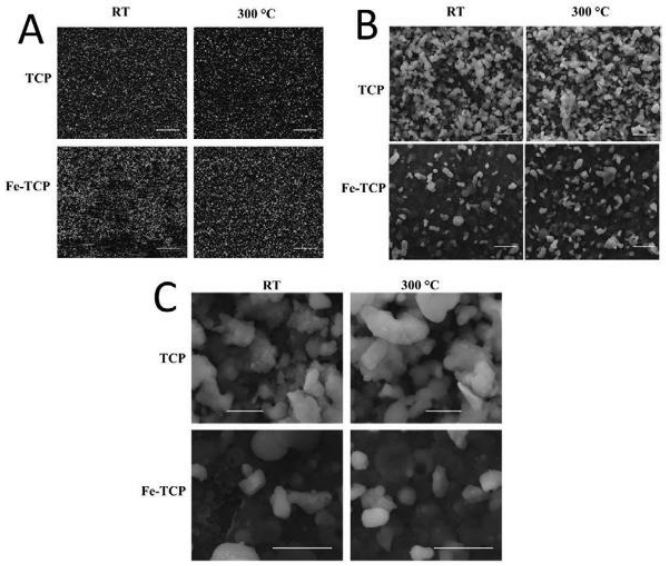

Figure 20: SEM micrographs of TCP and Fe-TCP thin films obtained by PLD at RT and 300 °C. Scale bar A) 50 μm, B) 20 μm, C) 3 μm (upper images) and 5 μm (lower images) [109].

A particular study revealed that Fe-TCP thin films, deposited on biodegradable Mg-Ca alloys using the PLD technique, demonstrated smoother microstructures compared to TCP coatings. SEM micrographs (Figure 20) showed that the presence of iron in the Fe-TCP coatings modified their structure and morphology, resulting in improved corrosion resistance and reduced degradation rates. Furthermore, the temperature set at 300°C was proved to be the best for the deposition process, as the Mg-Ca alloy coated with Fe-TCP at this particular temperature showed the highest protective efficiency in simulated body fluid and exhibited good cytocompatibility, inhibiting the growth of Escherichia coli [109].

5.1.4 Octacalcium phosphate thin films on titanium substrate

Titanium implants are widely used for load-bearing implants and inner fixation devices due to their relevant mechanical properties. Their integration with bone tissue depends on the physico-chemical characteristics of the implant/tissue interface [113]. The application and properties of Ti were mentioned before in Chapter 5.1.1.1.

Octacalcium phosphate (OCP) is related to calcium phosphate materials [114], it is a salt that is considered a precursor of bone and tooth apatite crystals [115]. When applied as a coating on metallic implants, OCP has been found to enhance osteoconductivity more compared to original surfaces like BCA or amorphous CA coating for example [116,117]. When synthetic OCP is implanted in bone defects, it undergoes a transformation into HA [118,119]. OCP stimulates the formation of osteoblastic cells, leading to improved bone formation, possibly through the formation of apatite and the conversion process itself [118,120]. Additionally, OCP-based materials have demonstrated the ability to promote osteoblastic cell differentiation in vitro [121] and potentially facilitate new bone formation in vivo, indicating osteotransductive properties [114]. Consequently, utilizing OCP material for coatings holds significant potential for enhancing the biological performance of metallic implants.

Mróz et al. performed the deposition of OCP film on the surface of 316L stainless steel [122]. Due to its mechanical characteristics, biocompatibility, and corrosion resistance, 316L stainless steel is regarded as one of the alluring metallic materials for biomedical applications [123]. The deposition process involved the use of an excimer ArF laser with a laser fluence of approximately 7 J/cm^2. 316L stainless steel acted as a substrate, which had a nanocrystalline diamond (NCD) buffer layer. The purpose of the NCD buffer layer was to combine materials with different structural and mechanical properties, allowing for better integration and performance. The substrate temperature during the process was controlled at 150 ± 30°C [122].

The deposited OCP layer showed a well-developed structure characterized by round-shaped grains measuring approximately 200 nm in size. The grains had different heights (Figure 21) while maintaining a homogeneous distribution across the surface [122].

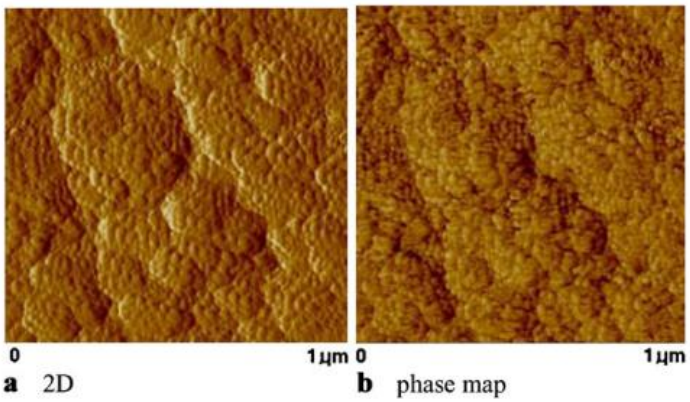

Figure 21: OCP deposited on 316L stainless steel with NCD buffer layer: (a) 2D AFM image, (b) phase map [122].

Cells culturing on the surface of OCP showed that obtained layers of OCP were deemed suitable for cultivating osteoblast cells [122].

In a research done by Smirnov et al., a new method for OCP thin films synthesis was developed. Because of the low temperature at which OCP's thermal disintegration occurs, it is generally known that this material is exceedingly challenging to deposit via direct physical methods. This method includes a combination of PLD and chemical treatment. They deposited $CaCO_3$ layer on Ti substrate using a Nd:YAG laser source with laser fluence fixed at 30 J/cm^2. During deposition, the Ti substrate was kept at room temperature, for a deposition time of 5 h. The CC coating, with a thickness of approximately 10 µm, exhibited strong adhesion to the Ti substrate and displayed a uniform appearance (Figure 22A). After obtaining CC coating, it was exposed to chemical treatment. Shortly CC films were transformed into dicalcium phosphate dihydrate (DCPD) ($CaHPO_4{\cdot}2H_2O$, Brushite) via a chemical soaking procedure in calcium nitrate solution for 168 h. The DCPD films were found to be thinner, measuring about 2 µm in thickness (Figure 22B). Further, the obtained DCPD films were transformed into OCP upon 168 h of soaking in sodium acetate. The final OCP films had a thickness of less than 1 µm (Figure 22C) [113].

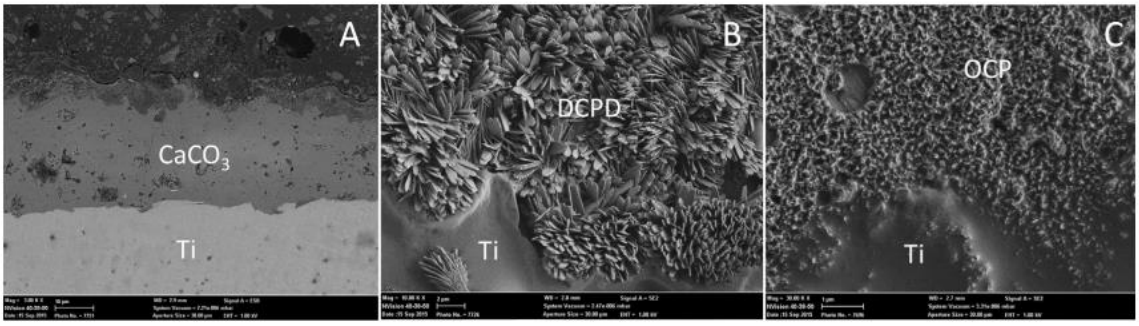

Figure 22: SEM images of the cross section of CC films (A); DCPD films (B) formed after CC soaking in calcium nitrate solution for 168 h and final OCP films (C) formed after DCPD soaking in sodium acetate for 168 h [113].

The films that were prepared displayed a consistent and smooth surface, devoid of cracks, indicating excellent adhesion to the Ti substrate. Furthermore, the OCP films exhibited higher rates of proliferation for both myofibroblasts and BMMSs (Bone Marrow Mesenchymal Stem Cells). This fact indicates that applying an OCP coating to titanium surfaces could create a favorable environment for successful osseointegration in clinical settings [113].

5.2 Bioactive glass and ceramic thin films

Bioactive glasses (BGs) belong to a unique category of biocompatible ceramics primarily composed of oxides. These glasses possess the ability to form bonds with both hard and soft tissues and simultaneously promote the growth of new tissue. Additionally, they gradually dissolve over time, making them highly desirable materials for applications in healthcare and regenerative medicine [124,125]. Larry Hench, a professor at the University of Florida, pioneered the invention of the first bioactive glass in 1969. Recognizing the issue of bioinertness with existing materials like metals and polymers, which led to fibrous encapsulation rather than a stable tissue interface, Professor Hench developed a degradable glass with a high calcium content to address this issue [126]. It was discovered that a glass of the composition 46.1 mol.% SiO_2, 24.4 mol.% Na_2O, 26.9 mol.% CaO and 2.6 mol.% P_2O_5, later termed 45S5 and Bioglass®, formed a bond with bone so strong that it could not be removed without breaking the bone [127]. The current knowledge indicates that the presence of inorganic ions released from the surface of the glass has an impact on cellular processes. Bioactive glasses have the ability to interact with living tissue, triggering a beneficial response that promotes healing, regeneration, and the growth of damaged or diseased tissue, particularly in the case of bone [128].

Bioactive glass is characterized by its amorphous structure, while glass-ceramics are crystallized glasses comprising a combination of crystalline and residual glassy phases. The bioactivity of 45S5 glass, specifically, is attributed to its compositional features. These include a lower SiO_2 content compared to more chemically durable silicate glasses, higher concentrations of Na_2O and CaO (acting as glass network modifiers), and a higher CaO/P_2O_5 ratio [129]. Research findings suggest that the bonding between 45S5 glass and bone occurs through the creation of a carbonate-substituted hydroxyapatite-like layer on the glass surface when in contact with bodily fluids. This CHA layer, resembling the mineral composition of natural bone, establishes a strong bond with living bone and tissue [130,131].

Currently, there exist various types of bioactive glass, including conventional silicate glasses like Bioglass 45S5, as well as phosphate-based glasses and borate-based glasses [129]. Remarkably, despite decades of extensive research conducted by multiple research groups, no alternative bioactive glass composition has been discovered to exhibit superior biological properties compared to the original Bioglass® composition [125].

A glass-ceramic refers to a type of glass that contains both micro- and nanocrystalline phases. There is no specific standard or norm that dictates the exact composition required to classify a material as glass-ceramic [132]. Extensive research has demonstrated that annealing bioactive glass to induce the formation of crystalline phases and transform it into glass-ceramic results in increased mechanical strength compared to glass. However, this enhanced mechanical strength comes at the cost of reduced bioactivity in the glass-ceramic form [133].

Pulsed Laser Deposition is among the various techniques employed for acquiring bioactive glass coatings [134]. When applying a bioactive glass coating, it is important to carefully control the thickness. BGs exhibit a rapid bioactive response, and an insufficient coating thickness can result in complete dissolution before the formation of a crystalline apatite layer. Conversely, overly thick coatings can negatively impact substrate adhesion due to stress accumulation. Therefore, finding the right balance is essential to ensure proper coating performance [135].

BGs have found wide application in the field of hard tissue engineering due to their remarkable bioactivity, osteoconductive properties, and ability to stimulate bone growth [133,136]. Another useful property of bioactive glasses is their ability to minimize the rapid corrosion of alloys. BGs exhibit a slower rate of biodegradation, which is accompanied by the advantageous release of trace elements that play a role in physiological biochemical cycles [137]. The next chapters will be dedicated to bioactive glasses and glass-ceramics film growth utilizing the PLD method on different substrates.

5.2.1 Bioactive glass thin films and coatings on titanium substrate

The application of Ti and its alloys as implants was mentioned in detail in Chapter 5.1.1.1 Another way to solve the problem of bioinertness and susceptibility to bacterial infections of titanium implants is to apply bioglass film. For PLD technique bioactive glass

system can be synthesized by the sol-gel method [131] or by mixing the powders of glass components [138].

Kwiatkowska et al. conducted bioactive glass coatings synthesis on Ti substrate. They used the Q-switched Nd:YAG laser, operating at 1064 nm with fluence 15 J/cm^2. The target used in the process was a melt-derived bioactive 42S5.2 Na-K glass of composition: 42.34 wt% SiO_2, 23.06 wt% CaO, 11.50 wt% Na_2O, 17.47 wt% K_2O, 5.63 wt% P_2O_5 with Ca/P molar ratio equal to 5,18. A polycrystalline titanium plate was employed as a substrate [139].

The material deposited by PLD exhibited uniform coverage on the titanium substrate. However, it was observed that small spherical particles, resembling droplets and measuring a few micrometers in diameter, were also present on the surface of the coating. It was reported that the bioactive glass, which was transferred from the target to the titanium substrate, retained its bioactive properties [139].

Sanz et al. conducted a study to investigate the influence of laser fluence on the morphology and roughness of deposited films. They utilized the third harmonic of an Nd:YAG laser at two laser fluences (50 and 100 mJ/cm^2), with a wavelength of 355 nm, to deposit a niobo-phosphate bioactive glass (NbP-BG) in a vacuum environment [140]. Niobium was chosen as a doping element as it has been found that Nb has the potential to enhance both the mechanical and biological properties of synthetic implants [141]. Niobium-doped bioactive glass has shown promising results in stimulating the formation of new bone tissue in areas with bone defects [142]. Furthermore, when compared to other metal ions (e.g., Ag, Sr, Cu, Nb), niobium has been reported to exhibit lower cytotoxicity and the ability to improve the mineralization process in human osteoblast populations [143]. Through the use of SEM and AFM analysis on films produced under these two different conditions (Figure 23), it can be observed that higher laser energy resulted in a greater number of larger droplets on the films, leading to increased roughness values. The researchers attributed the presence of these droplets to a splashing mechanism observed during the ablation process, which typically intensifies with higher laser energy [140].

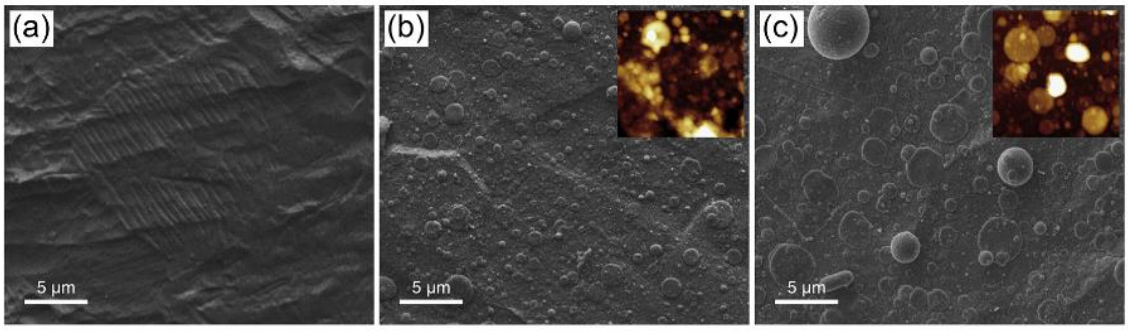

Figure 23: SEM images (a) Titanium substrates; NbP-BG thin films deposited on Titanium substrates deposited (b) 50 mJ/cm^2 and (c) 100 mJ/cm^2 laser fluence, 10000× magnification. AFM inserts are at the same scale of figures. Modified by [140].

5.2.2 RKKP glass-ceramic thin films on titanium substrate

RKKP (stands for Ravaglioli, Krajewski, Kirsch and Piancastelli) [144] is a bioactive glass-ceramic system of the composition 43.68 SiO_2, 11.10 P_2O_5, 31.30 CaO, 4.53 Na_2O, 2.78 MgO, 4.92 CaF_2, 0.19 K_2O, 0.50 La_2O_3, 1.00 Ta_2O_5, in wt% [33]. The RKKP shows significant promise as a glass-ceramic material due to its impressive biological properties, such as excellent biocompatibility and the ability to support bone growth. Extensive research has demonstrated its high bioactivity and osteoconductive properties [145]. In vitro experiments have shown that fibroblasts and osteoblasts exhibit favorable responses when exposed to solid RKKP pellets, while in vivo studies have shown their ability to bond not only with healthy bone but also with osteopenic bone [146].

Rau et al. conducted a deposition of glass-ceramic thin films from the RKKP target on Ti substrate. As the ablation laser source doubled Nd:YAG laser was used with a laser fluence 12 J/cm^2. The experiment was carried out in a high vacuum. In this work, two different RKKP targets, prepared by the melt-processing and the sol-gel synthesis routes were applied [33].

From the SEM images it is clear that while both films share a compact, dense, and relatively uniform morphology, the film obtained through melt processing displays sporadic droplets on its surface (Figure 24A). On the other hand, the sol-gel coating exhibits a highly compact and smoother surface(Figure 24B). These notable differences in morphology suggest that the deposition process in PLD is influenced by the preparation procedure of the target material [33].

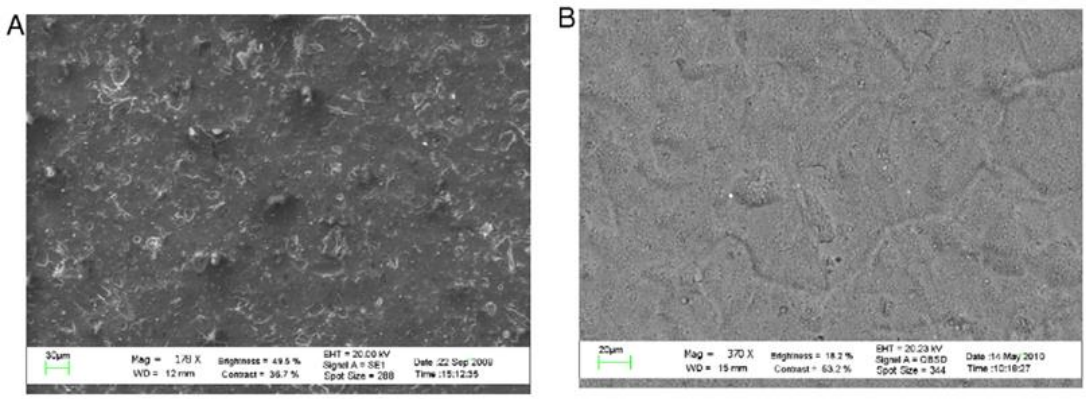

Figure 24: SEM micrographs of film deposited at 500 °C: (A) from the melt-processing RKKP target and (B) from the sol-gel RKKP target [33].

Despite the film deposition conditions being nearly identical, the difference in thickness between the two types of films is also noted: the film derived from the melt-processing target has a thickness of 0.6 ± 0.1 μm, whereas the film obtained from the sol-gel target is much thicker, measuring 4.3 ± 0.3 μm [33].

Presented research demonstrated that the optimal parameters for depositing RKKP films via PLD are a laser fluence of 12 J/cm^2 and a temperature of 500 °C. These specific conditions enable the deposition of crystalline films with a composition that closely resembles that of the initial targets. The films obtained under these conditions exhibit a compact and uniform microstructure, significantly improved mechanical properties, and varying surface roughness depending on the type of target used [33].

5.2.3 Cu-containing bioactive glass/eggshell membrane nanocomposites

Copper-containing bioactive glass/eggshell membrane nanocomposites have been utilized to enhance the processes of angiogenesis, antibacterial effectiveness, and wound healing [147]. The inclusion of Cu^{2+} ions in the bioactive glass was specifically selected because of their capacity to stimulate angiogenesis [148], in addition to their established antimicrobial properties against Escherichia coli, methicillin-resistant Staphylococcus aureus, and Clostridium difficile [149].

Chapter 5.2 discusses the utilization of bioactive glasses in the field of hard tissue engineering. However, more recently, there has been a growing interest in exploring the potential of bioactive glasses for interacting with soft tissues and promoting wound healing. These studies encompass various areas such as vascularization, cardiac, lung, nerve,

gastrointestinal, and laryngeal tissue repair [129,150,151], indicating a broadening scope for the application of bioactive glasses in these contexts.

Eggshell membrane (ESM) is a thin fibrous connective tissue consisting of inner and outer layers, with a typical thickness ranging from 60 to 80 μm. It is primarily composed of collagen, making it highly collagenized [152]. ESM is an inexpensive material that is easily obtainable, and it possesses a high level of biosafety. Being a natural substance, ESM exhibits a porous structure with a biopolymeric fibrous network, with proteins comprising around 80-85% of its composition. Collagens, make up approximately 10% of the fibers present in ESM. One of the remarkable features of ESM is its porous and fibrous structure, which provides it with a large surface area, promotes reasonable adhesion and allows for gaseous exchange. Moreover, the antibacterial properties of ESM, which are important for wound healing, have been confirmed in previous studies [153].

There are three notable advantages of PLD that encourage the choice of this particular technique for work with ESM. firstly, Its highly energetic nature enables in situ synthesis of uniform nanocomposite coatings [154]. This eliminates the issues of inhomogeneity and instability commonly associated with other conventional modification methods. Another advantage of PLD is its ability to prepare nanocoatings without requiring additional heat treatment. This allows for the preservation of the porous fibrous structure in materials like eggshell membrane while maintaining the activity of collagen [155]. Additionally, the deposition time in PLD can be adjusted to easily control the thickness of the nanocoatings, providing flexibility in tailoring the coatings according to specific requirements [147].

Li and co-workers prepared Cu-BG film on an eggshell membrane using PLD. The as-sintered Cu-containing glass-ceramic discs with different Cu contents (0.2 and 5 mol%) were used for the target materials. They were synthesized by a sol-gel method. ESM films acted as substrates. The Cu-containing glass-ceramic discs were ablated using focused laser fluence of 71 kJ/cm^2. The ambient O_2 was used as a background gas with a pressure of 20 MPa and a treating time of 40 min [147].

SEM analysis demonstrated that the pure eggshell membrane film surface (Figure 25 a, b) exhibited a fibrous structure with smooth fiber surfaces. Following a 40-minute PLD process, where xCu-BG was applied as a coating, a uniform nanocoating of xCu-BG comprising consistent nanosized particles was observed on the surface of the ESM films [147].

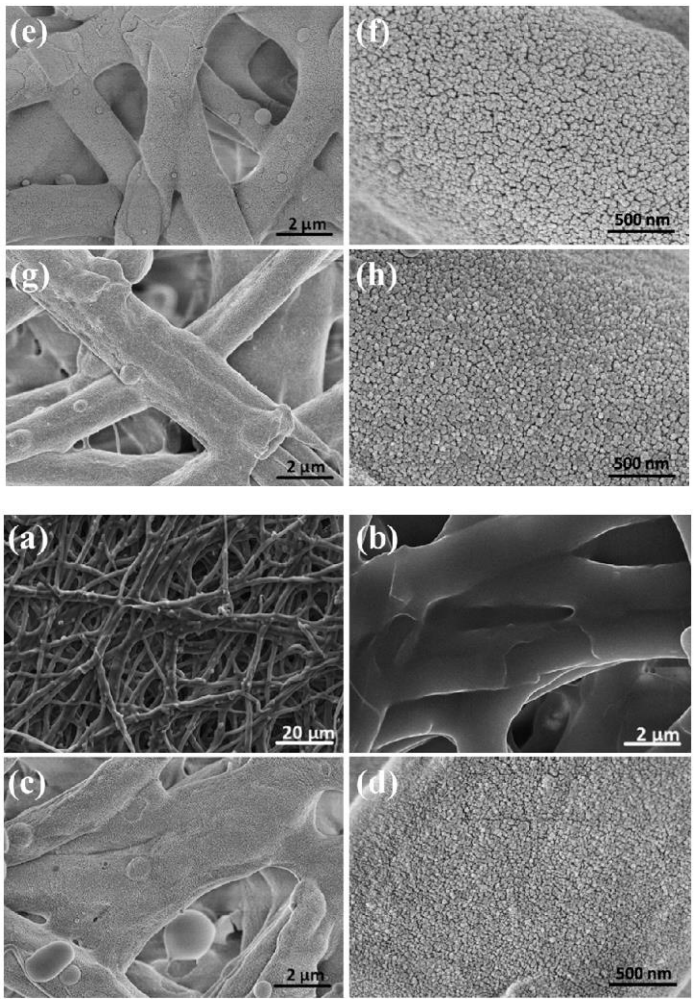

Figure 25: SEM analysis of the xCu-BG nanocoating on the surface of ESM films by the PLD technique. Outer ESM (a, b), 0Cu-BG/ESM (c, d), 2Cu-BG/ESM (e, f), 5Cu-BG/ESM (g, h). (a, c, e, and g) are low-magnification images, and (b, d, f, and h) are high-magnification images [147].

Notably, the ESM films retained their fiber-like microstructure even after the coating process (Figure 25 c-h) [147].

Cu-BG/ESM films obtained during particular research exhibited remarkable enhancements in surface physicochemical properties, antibacterial activity, and angiogenic potential in both in vitro and in vivo experiments. These facts indicate that the PLD-prepared Cu-BG/ESM nanocoatings can be effectively used for wound healing applications [147].

5.3 Diamond-like Carbon thin films

Enhancing the body's acceptance of prostheses can be achieved by applying a biocompatible coating to the implants. Over the last ten years, apart from other materials carbon has emerged as a highly suitable material for such coatings in medical contexts. Carbon has

proven to possess excellent biocompatibility, likely attributable to its fundamental role as a foundational element in all organic systems [156]. Carbon is a unique element. It is able to form tetrahedral (sp3), trigonal (sp2), and linear (sp1) bond coordinations. A wide array of both natural and synthetic forms of carbon exist, encompassing diamond, graphite, fullerenes, nanotubes, and diamond-Like carbon (DLC). These materials represent just a fraction of the diverse range of carbon-based substances available [157].

Diamond-like carbon is a term used to describe a metastable phase of amorphous carbon, encompassing a class of hard carbon-based materials [158]. DLC films are amorphous coatings composed of a blend of sp2 (graphite-like) and sp3 (diamond-like) bonds of carbon atoms, with varying ratios and the potential inclusion of hydrogen. The characteristics of DLC coatings are significantly influenced by the amount of hydrogen present and the ratio of sp3 to sp2 bonds, which, in turn, depends on the deposition process and its parameters [156,159,160]. In recent times, DLC films have gained significant biomedical applications, particularly in situations that demand low cell adhesion [161,162]. DLC coatings are highly appealing as biomedical coatings because of their unique physiochemical, mechanical, and tribological properties [163,164]. They exhibit corrosion resistance [165], exceptional biocompatibility [157,166], high hardness, low friction coefficient, and low wear rates [157]. These characteristics make DLC coatings well-suited for medical applications, particularly in artificial implants like hip and knee joints [167], bone plates [168], heart valves [162,169], heart diaphragms [162,171], catheters [171], stents [172], and splints [173].

PLD is one of the several types of deposition techniques employed for synthesizing DLC films. The initial attempt to grow DLC films using pulsed laser deposition was documented in the 1980s [174]. An advantage of using pulsed laser deposition for DLC coatings is its ability to provide sufficient energy (approximately 100 eV) to the carbon ions in the plasma. This energy facilitates the transition from the hybridized sp2 bond to the hybridized sp3 bond, as proposed by the subplantation model of DLC film growth [175]. Additionally, PLD enables control over the composition of the deposited film. By utilizing a hydrogen-containing target or introducing a hydrogen-containing gas, PLD can yield hydrogenated DLC films, whereas, without these factors, it typically produces non-hydrogenated DLC films [176]. Hydrogenated DLC can be characterized as a highly dense polymer. These films consist of an amorphous carbon matrix with a hydrogen content of up to 30 atom % and oxygen content of up to 10 atom % [157]. Non-hydrogenated DLC films generally demonstrate greater hardness when compared to hydrogenated DLC films [177], higher thermal stability [178], and higher physical and

chemical inertness [176]. PLD offers several other advantages, such as the ability to co-ablate different materials for doping or alloying DLC films [174]. It allows for the deposition of DLC films at low temperatures [179,180], enables micro-area deposition, and facilitates in situ introduction of gases during the process [174]. PLD is not as widely utilized as other technologies, likely due to the challenge of achieving uniform film growth, which is attributed to the directional nature of laser-induced plasma. One approach to partially overcome this limitation is to introduce substrate rotation or motion during the deposition process. However, the versatility of PLD enables the deposition of doped or alloyed DLC films, even beyond the solubility limits, offering opportunities for exploring unconventional compositions [157,174].

Pulsed laser deposition of DLC is a direct and uncomplicated process that entails ablating a carbon-containing target, leading to the formation of a film containing a certain proportion of sp3-hybridized carbon atoms. The commonly employed target material is high-purity graphite, although other materials such as pressed diamond powder, glassy carbon, and polycarbonate have also been used as targets [157]. Incorporating additional materials offers the possibility of fine-tuning the properties of DLC films to meet specific application requirements. The fundamental process of solid doping in PLD can be accomplished through three methods: sintering graphite and doping material powders into a doped target [181], a doping patch is inlaid onto/into the graphite target [182,183], or an independent graphite target and doping material target are alternately ablated by the laser beam [184].

While DLC films possess various properties, the hybridized sp3 bond content stands out as the most significant characteristic [185]. By conducting depositions of DLC films using various laser wavelengths: 193 nm [186], 248 nm [186,187], 532 nm [188], 1064 nm [179], and 800 nm [189] with various fluences, it became apparent that reducing the laser wavelength (except for 780-800 nm) or increasing the fluence leads to an elevated sp3 content in the DLC films [174]. A KrF excimer laser with a 248 nm wavelength is most widely used for the growth of DLC films by PLD, it can achieve a high sp3 content (above 80%) at relatively low fluences (around 8-20 J/cm^2). However, when the highest laser fluence (80 J/cm^2) is utilized, it results in a lower sp3 content (approximately 60%) in the DLC films [191,191].

The incorporation of a suitable ambient gas can enhance the characteristics of DLC films. By introducing a moderate ambient gas during the process, the properties of the laser-induced plume, such as quality, species, distribution, and kinetic energy, can be significantly altered [192,193]. As a background gas, both inert and reactive gases can be used. In

comparison to inert gases like argon and helium, reactive gases such as hydrogen or hydrogenated gas (C_2H_2 and CH_4), oxygen, and nitrogen undergo partial ionization and actively contribute to the formation of DLC films. These elements can also be doped into the DLC film during the deposition process. Hydrogen plays a vital role in defining the tribological, optical, and mechanical properties of DLC films [174]. Using hydrogen as an ambient gas results in the formation of hydrogenated DLC (HDLC) films, which were mentioned earlier. Deposition of DLC coatings in the O_2 atmosphere results in the formation of O-doped DLC films. However, the hardness of these films decreases primarily due to two factors: porosity, which reduces the film density, and the substitution of C-C sp3 bonds with C-O bonds [194]. The use of nitrogen results in the dissociation of nitrogen molecules, facilitated by the collision between carbon species and nitrogen. This dissociation allows nitrogen to actively participate in the formation of N-doped DLC films [174]. The involvement of nitrogen verifies the electrochemical activity, tribological, and photoluminescence properties of DLC films [195], and effectively releases the internal stress in the films [196]. In the upcoming chapters, the focus will be on the examples of growth of DLC films through the employment of the PLD method.

5.3.1 Ag-incorporated Diamond-like Carbon thin films

DLC coatings can be enhanced in their biological performance by incorporating Ag [197]. The presence of Ag in DLC coatings enables the release of metal ions, which exhibit antimicrobial properties [198] and contribute to reducing the clot-forming potential of artificial implants like coronary stents [199]. Consequently, Ag is extensively employed to enhance various biomedical aspects of DLC coatings, including biocompatibility [200], genotoxicity [201], antimicrobial activity, hemocompatibility [202], and inhibition of bacterial and tumor growth [203]. To maintain biocompatibility and prevent cytotoxicity, DLC coatings should be carefully designed with an optimal amount of Ag doping. This ensures effective antimicrobial protection without harming human cells during their service life [204]. Ag-DLC can be applied as a coating for joint implants to improve its mechanical, biological and antibacterial properties [200].

Various techniques were employed to prepare Ag-DLC films, with different representations of silver, for the purpose of studying their antibacterial properties against various types of bacteria [202,205,206]. When the films contained a high concentration of silver, the results consistently demonstrated an antibacterial effect of more than 80% [202,205].

On the other hand, the antibacterial impact varied greatly when the silver concentration was low, from 10% to 90% [206].

In the research done by Písařík and co-workers a dual pulsed laser deposition technique (dual-PLD - two lasers, two targets) was utilized to deposit Ag-DLC coatings. The deposition process involved employing two KrF excimer lasers with a wavelength of 248 nm. One laser was directed toward a high-purity graphite target with an energy density of 8 J/cm^2, while the second laser was focused on a silver target with an energy density of 5 J/cm^2. The entire deposition process took place at room temperature, and argon was used as the ambient gas. By varying the deposition parameters, the Ag content in the resulting films ranged from 1.1 at% to 9.3 at%, while the silver concentration on the film surface varied from 1.4 at% to 7.9 at%. The AFM analysis revealed an increase in surface roughness as the silver content in the films increased. It is worth noting that the roughness parameters exhibited variations across different locations on the sample, indicating some degree of surface irregularity or heterogeneity [197].

The study demonstrated that as the silver content increased in the Ag-DLC films, there was a notable increase in the proportion of sp2 contribution, while the proportion of sp3 contribution decreased from 81% to 36%. This resulted in an increased sp2/sp3 ratio with higher silver concentrations [197]. Previous research by Zhang had also shown that silver doping reduced the sp3 content in hydrogen-free DLC, while the sp2/sp3 ratio remained relatively constant in hydrogenated DLC [207]. Similarly, Ahmed observed similar trends in hydrogen-free DLC [208]. The findings of Písařík et al. aligned with these previous studies, indicating that silver doping leads to a decrease in the diamond-like carbon content and an increase in the graphitic carbon content in the Ag-DLC films [197].

To summarize, Ag-DLC layers with the highest silver content (9.3 at%) showed strong antibacterial efficacy. Písařík and co-workers study revieled that after 3 hours, they achieved 98.6% efficiency against Pseudomonas aeruginosa and 81.6% against Staphylococcus aureus. After 24 hours, the efficiency increased to nearly 100% for both types of bacteria. Such results are confirming that PLD is an applicable method for the preparation of Ag-DLC thin films for medical purposes [197].

5.3.2 Diamond-like Carbon coating of textile blood vessels

In Chapter 5.3 was mentioned the notable hemocompatibility and reduced risk of thrombus formation associated with DLC thin films. Heart valves and stents with DLC coating are already commercially available [209]. Polyethylene, polyurethane, textile, and other materials are commonly used to fabricate artificial blood vessels, which have inner diameters ranging from several tenths of microns to several millimeters. The application of a coating to these tubes reduces the likelihood of thrombosis formation and enhances their compatibility with living tissue surfaces [156].

Research conducted on animal models has demonstrated that stents coated with DLC thin film are more effective in preventing the development of intimal hyperplasia compared to uncoated stents [210]. Controlled studies conducted on human subjects have also yielded similar findings, confirming the superiority of DLC-coated stents in this regard [211].

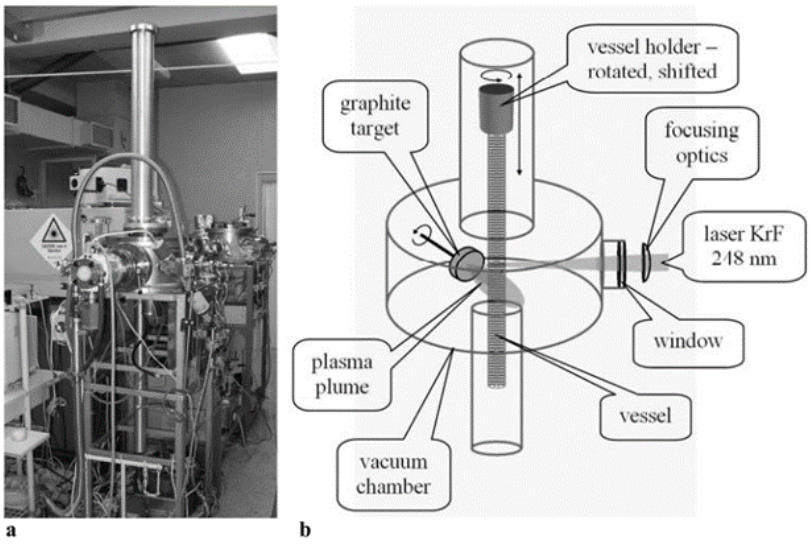

Figure 26: Deposition system for coating of textile blood vessels: a photo of a vertical coating system, b scheme of the deposition system [156].

Kocourek and co-workers conducted a study to examine the coating process of artificial textile blood vessels with hydrogen-free amorphous DLC layers. The films were produced using PLD with a KrF excimer laser (λ = 248 nm). A high-purity graphite target was used to ablate the carbon species, with the laser beam energy density on the target ranging from 10 to 20 J/cm^2. The deposition of the DLC layers was carried out either in a vacuum or in an argon environment. For in vivo tests, textile blood vessels served as the substrate (Figure 27). In this setup, the carbon material being deposited passed through the tube, covering both the inner and

outer surfaces. Importantly, the DLC layers were applied at room substrate temperature to prevent any damage to the vessel material during the coating process [156].

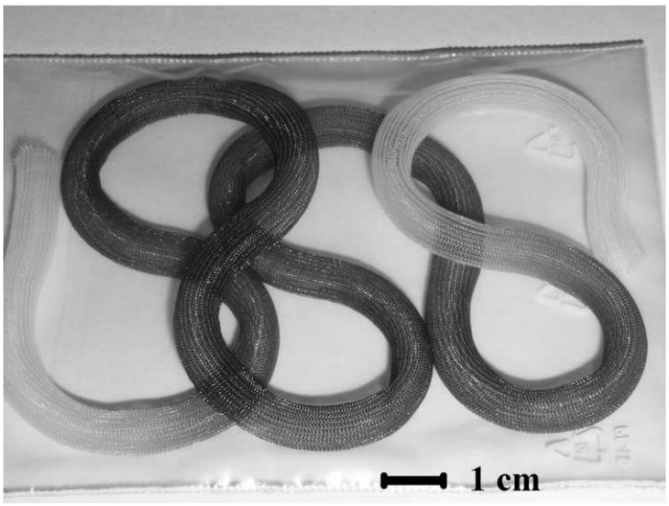

Figure 27: DLC-coated textile blood vessel of 7 mm diameter and 30 cm length (created in 0,25 Pa of argon, 20 J/cm^2) [156].

The deposited DLC films demonstrated excellent biocompatibility. The results obtained from the in vivo experiments of films with different DLC thicknesses, indicated that the performance of the films was not significantly influenced by the type or thickness of the DLC layers [156].

5.3.3 Si-incorporated Diamond-like Carbon thin films

Silicon-infused carbon coatings not only show decreased internal stress but also possess superior mechanical [212], tribological [213,214], corrosion [214] and biological properties [215]. Regarding the biocompatibility of Si-DLC coatings, research has shown that higher concentrations of silicon promote the adherence of human endothelial cells [215]. Furthermore, experiments conducted by Okpalugo et al. verified that Si-DLC coatings do not display any toxic effects on these cells [216,217].

It has been proposed that incorporating silicon into the DLC matrix can potentially enhance the osseointegration process [218]. Silicon plays a vital role in bone calcification, enhancing bone density and inhibiting osteoporosis. It is essential for the metabolic processes associated with bone formation, particularly during the initial stages, promoting osteogenesis [219]. In addition to the positive qualities mentioned earlier, Eisinger et al. demonstrated that silicon induced a notable rise in femoral bone mineral density in women with osteoporosis

[220]. Furthermore, it has been observed that Si-DLC coatings can achieve a slight improvement in the adhesion and proliferation of osteoblasts [218]. Si-DLC coatings also offer the advantage of high hemocompatibility, enabling appropriate interaction between the surface of the implant and blood [221,222,223]. It was proved that a higher silicon content is correlated with a reduced number of platelets adhering to the surface [221]. Okpalugo et al. conducted experiments that showed a decrease in the formation of platelet aggregates on Si-doped DLC coatings [222,223].

H. Nakazawa et al. performed the deposition of Si-DLC coatings in their study. They used two types of targets: a graphite target (99.9%) and 10% and 20% Si-containing C targets. The purpose was to deposit unhydrogenated and hydrogenated Si-DLC films in order to examine their structure, mechanical properties, and tribological properties. The substrate utilized for deposition was a Si wafer. A KrF excimer laser with a wavelength of 248 nm was employed to ablate the targets. The laser parameters were set to a fixed repetition rate of 20 Hz and a power of 0.25 J/pulse. Additionally, hydrogen gas was introduced into the chamber to generate atomic hydrogen for the synthesis of hydrogenated films [224].

Summarizing, the deposition of Si-DLC coatings was accomplished successfully. Results of described research showed that the critical loads of the films deposited with hydrogen were observed to be higher compared to those deposited without hydrogen. Furthermore, it was discovered that the Si-DLC films subjected to hydrogen irradiation exhibited a tendency towards enhanced wear resistance in comparison to the unhydrogenated Si-DLC films [224].

6 Conclusion

This thesis has provided a comprehensive study of the use of pulsed laser deposition for the preparation of thin films in the context of medical materials. Through the study the significant contribution of PLD in advancing the field of medical materials manufacturing was emphasize.

Firstly, the principles of PLD operation were thoroughly studied, including the interaction of the laser with the material, the dynamics of ablation and the expansion of the plume. Understanding these mechanisms is important for optimization the deposition process and achieving the desired film properties. The study of the process parameters, such as laser fluence, substrate temperature, ambient gas pressure and etc., revealed their strong influence on the growth, morphology and crystallinity of thin films. This knowledge allows to change the properties of the film in accordance with specific medical applications.

The successful implementation of PLD in the production of medical devices and implants was demonstrated through specific case studies. These studies have showed the ability of PLD films to promote cell adhesion, proliferation, non-toxicity and hemocompatibility, making them suitable for biomedical applications. Performance evaluations of PLD-based thin films have demonstrated their effectiveness in real-world applications, showing increased productivity, biocompatibility and patient treatment outcomes. These results open up promising prospects for the development of medical technologies and improved patient care.

Overall, this thesis highlighted the significant contribution of PLD to the production of thin films for medical materials. The precise control of the composition, thickness and structure of the film provided by PLD allows the development of coatings with exceptional properties and functionality. These advances have the potential to revolutionize the production of medical equipment, which contributes to improved treatment outcomes and improved patient care.

In the future, further researches may be aimed at optimizing PLD processes, exploring new materials and surface modifications, as well as studying the long-term biocompatibility and performance characteristics of thin films obtained using PLD. By continuing to deepen our understanding and use of PLD in medical materials, we can drive innovation, shape future medical technologies, and ultimately improve the quality of healthcare worldwide.

7 Literature

[1] NORTON, David P. Pulsed Laser Deposition of Complex Materials: Progress Toward Applications. In: EASON, Robert, ed. Pulsed Laser Deposition of Thin Films. Hoboken, NJ, USA: John Wiley & Sons, Inc., **2006**, pp. 3-28. ISBN 9780470052129.

[2] OJEDA-G-P, Alejandro, DÖBELI, Max, LIPPERT, Thomas. Influence of Plume Properties on Thin Film Composition in Pulsed Laser Deposition. *Advanced Materials Interfaces*. **2018**, 5(18), 1701062.

[3] DUTA, Liviu and POPESCU, Andrei C. Current Research in Pulsed Laser Deposition. *Coatings*. **2021**, 11(3), p.274.

[4] RAU, Julietta V., GENEROSI, Amand A, LAURETI, Sara, KOMLEV, Vladimir S., FERRO, Daniela, CESARO NUNZIANTE, Stella, PACI, Barbara, ALBERTINI ROSSI, Valerio, AGOSTINELLI, Elisabetta and BARINOV, Sergey M. Physicochemical Investigation of Pulsed Laser Deposited Carbonated Hydroxyapatite Films on Titanium. *ACS Applied Materials & Interfaces*. **2009**, 1(8), pp.1813-1820.

[5] DI FONZO, F., TONINI, D., LI BASSI, A., CASARI, C. S., BEGHI, M. G., BOTTANI, C. E., GASTALDI, D., VENA, P. & CONTRO, R. Growth regimes in pulsed laser deposition of aluminum oxide films. *Applied Physics A*. **2008**, 93, pp.765-769.

[6] OGUGUA, Simon N., NTWAEABORWA, Odireleng, M. and SWART, Hendrik, C. Latest development on pulsed laser deposited thin films for advanced luminescence applications. *Coatings*. **2020**, *10*(11), 1078.

[7] DEEPAK, Marla, UPENDRA, Bhandarkar V., SUHAS, Joshi S. Critical assessment of the issues in the modeling of ablation and plasma expansion processes in the pulsed laser deposition of metals. *Journal of Applied Physics*. **2011**, 109(2), p.021101.

[8] SHEPELIN, Nick A., TEHRANI, Zahra P., OHANNESSIAN, Natacha, SCHNEIDER, Christof W., PERGOLESI, Daniele and LIPPERT, Thomas. A practical guide to pulsed laser deposition. *Chemical Society Reviews*. **2023**, 52, pp.2294-2321.

[9] FUJIOKA, Hiroshi. Pulsed Laser Deposition (PLD). In: KUECH, Thomas F. ed. Handbook of Crystal Growth. 2Ed [online]. North-Holland: Elsevier B.V., **2015**, pp.365-397. ISBN 9780444633040.

[10] MORINTALE, E., CONSTANTINESCU, C. and DINESCU, M. Thin films development by pulsed laser-assisted deposition. *Physics AUC*. **2010**, 20(1), pp.43-56.

[11] RIJNDERS, Guus and BLANK, Dave H. A. In Situ Diagnostics by High-Pressure RHEED During PLD. In: EASON, Robert, ed. Pulsed Laser Deposition of Thin Films [online]. Hoboken, NJ, USA: John Wiley & Sons, Inc., **2006**, pp. 85-97. ISBN 9780470052129.

[12] O'MAHONY, Donagh and LUNNEY, James G. Group III Nitride Growth. In: EASON, Robert, ed. Pulsed Laser Deposition of Thin Films [online]. Hoboken, NJ, USA: John Wiley & Sons, Inc., **2006**, pp.291-308. ISBN 9780470052129.

[13] MOHOLKAR, A. V., SHINDE, S. S., BABAR, A. R., SIM, K. U., KWON, Y. B., RAJPURE, K. Y., PATIL, P. S., BHOSALE, C. H. and KIM, J. H. Development of CZTS thin films solar cells by pulsed laser deposition: influence of pulse repetition rate. *Solar Energy*. **2011**, 85(7), pp.1354-1363.

[14] CHRISTEN, H. M. and ERES, G. Recent advances in pulsed-laser deposition of complex oxides. *Journal of Physics: Condensed Matter*. **2008**, 20(28), 264005.

[15] SCHOU, J. Physical aspects of the pulsed laser deposition technique: The stoichiometric transfer of material from target to film. *Applied Surface Science*. **2009**, 255(10), 5191-5198.

[16] PRYDS, Nini, SCHOU, Jørgen, LINDEROTH, Søren. The spatial thickness distribution of metal films produced by large-area pulsed laser deposition. *Applied Surface Science*. **2007**, 253(19), pp.8231-8234.

[17] VOEVODIN, Andrey A., ZABINSKI, Jeffrey S., and JONES, John G. Pulsed Laser Deposition of Tribological Coatings. In: EASON, Robert, ed. Pulsed Laser Deposition of Thin Films [online]. Hoboken, NJ, USA: John Wiley & Sons, Inc., 2006, pp.585-608. ISBN 9780470052129.

[18] SCHOUS, J. Laser beam–solid Interactions: Fundamental aspects. In: PAULEAU, Yves. Materials Surface Processing by Directed Energy Techniques. 1st Edition. Great Britain: Elsevier Science, **2006**, pp. 35-66. ISBN 9780080458960.

[19] VANALAKAR, S. A., AGAWANE G. L., SEUNG, W. S., SURYAWANSHI, M. A review on pulsed laser deposited CZTS thin films for solar cell applications. *Journal of Alloys and Compounds*. **2015**, 619, 109-121.

[20] YAO, Xiong, MOON, Jisoo, CHEONG, Sang-Wook & OH, Seongshik. Structurally and chemically compatible BiInSe3 substrate for topological insulator thin films. *Nano Research*. **2020**, 13, pp.2541-2545.

[21] ZHU, B. L., ZHAO, X. Z., SU, F. H., LI, G. H., WU, X. G., WU, J. and WU, R. Low temperature annealing effects on the structure and optical properties of ZnO films grown by pulsed laser deposition. *Vacuum*. **2010**, 84(11), pp.1280-1286.

[22] GREER, Jim. Large-Area Commercial Pulsed Laser Deposition. In: EASON, Robert, ed. Pulsed Laser Deposition of Thin Films [online]. Hoboken, NJ, USA: John Wiley & Sons, Inc., 2006, pp.191-213. ISBN 9780470052129.

[23] NAZABAL, Virginie and NĚMEC, Petr. Amorphous thin film deposition. In: MUSGRAVES, David J., HU, Juejun, CALVEZ, Laurent, Eds. Springer Handbook of Glass. Switzerland: Springer, **2019**, pp. 1291-1324. ISBN 9783319937281.

[24] LE, Phuoc H. and LUO, Chih W. Thermoelectric and topological insulator bismuth chalcogenide thin films grown using pulsed laser deposition. In: YANG, Dongfang. Applications of Laser Ablation-Thin Film Deposition, Nanomaterial Synthesis and Surface Modification. Canada: IntechOpen, **2016**, pp.55-84. ISBN 9789535128120.

[25] KHAZAKA, Rami. From atomic level investigations to membrane architecture: An in-depth study of the innovative 3C-SiC/Si/3C-SiC/Si heterostructure. Doctoral thesis. François-Rabelais university of Tours, 2016.

[26] RIJNDERS, Guus and BLANK, Dave H. A. Growth Kinetics During Pulsed Laser Deposition. In: EASON, Robert, ed. Pulsed Laser Deposition of Thin Films [online]. Hoboken, NJ, USA: John Wiley & Sons, Inc., 2006, pp.177-190. ISBN 9780470052129.

[27] GREENE, J. E. Thin Film Nucleation, Growth, and Microstructural Evolution: An Atomic Scale View. In: MARTIN, Peter M. Handbook of Deposition Technologies for Films and Coatings - Science, Applications and Technology. 3rd Edition. William Andrew Publishing, **2010**, pp. 555-558. ISBN 9780815520320.

[28] AQUAL, J. N., BERBEZIER, I., FAVRE, L., FRISCH, T., RONDA, A. Growth and self-organization of SiGe nanostructures. *Physics Reports.* **2012**, 522, pp.60-179.

[29] MCMITCHELL, Sean R. C. An investigation into controlling the growth modes of ferroelectric thin films using pulsed laser deposition and RHEED. Doctoral thesis. University of Birmingham, 2008.

[30] GREER, James A. History and current status of commercial pulsed laser deposition equipment. *Journal of Physics D: Applied Physics*. **2014**, 47(3), p. 034005.

[31] DELMDAHL, R. and PÄTZEL, R. Pulsed laser deposition—UV laser sources and applications. *Applied Physics A: Materials Science and Processing*. **2018**, *93*, pp.611-615.

[32] NELEA, Valentina, MIHAILESCU, Ion N. and JELÍNEK Miroslav. Biomaterials: New Issues and Breakthroughs for Biomedical Applications. In: EASON, Robert, ed. Pulsed Laser Deposition of Thin Films [online]. Hoboken, NJ, USA: John Wiley & Sons, Inc., 2007, pp. 421-456. ISBN 9780470052129.

[33] RAU, J. V., TEGHIL, R., FOSCA, M., DE BONIS, A., CACCIOTTI, I., BIANCO, A., ROSSI, Albertini, V., CAMINITI, R. and RAVAGLIOLI, A. Bioactive glass-ceramic coatings prepared by pulsed laser deposition from RKKP targets (sol-gel vs melt-processing route). *Materials Research Bulletin.* **2012**, 47(5), pp.1130-1137.

[34] JINKER, Rüdiger, DIMAKIS, Athanasios and THONEICK, Maurice. Effects of implant surface coatings and composition on bone integration: a systematic review. *Clinical oral implants research*. **2009**, 20(s4), pp.185-206.

[35] MARLA, Deepak, BHANDARKAR, Upendra V. and JOSHI, Suhas S. Critical assessment of the issues in the modeling of ablation and plasma expansion processes in the pulsed laser deposition of metals. *Journal of Applied Physics.* **2011**, 109(2), p.021101.

[36] GITTARD, S. D., NARAYAN, R. J., JIN, C., OVSIANIKOV, A., CHICHKOV, B. N., MONTEIRO-RIVIERE, N. A., STAFSLIEN, S. and CHISHOLM, B. Pulsed laser deposition of antimicrobial silver coating on Ormocer® microneedles. *Biofabrication,* **2009**, 1(4), p.041001.

[37] KWONG, H. Y., WONG, M. H., WONG, Y. W. and WONG, K. H. Superhydrophobicity of polytetrafluoroethylene thin film fabricated by pulsed laser deposition. *Applied surface science*. **2007**, *253*(22), pp.8841-8845.

[38] RAMAY, Hassna R. R. and ZHANG, M. Biphasic calcium phosphate nanocomposite porous scaffolds for load-bearing bone tissue engineering. *Biomaterials*. **2004**, 25(21), pp.5171-5180.

[39] LEÓN, Betty. Pulsed Laser Deposition of Thin Calcium Phosphate Coatings. In: LEÓN, B. and JANSEN, J.A. Ed. Thin Calcium Phosphate Coatings for Medical Implants [online]. New York, USA: Springer, 2009, pp. 101-157. ISBN: 9780387777184.

[40] SURMENEV, R. A., SURMENEVA, M. A., EVDOKIMOV, K. E., PICHIGIN, V. F., PEITSCH, T. and EPPLE, M. The influence of the deposition parameters on the properties of an rf-magnetron-deposited nanostructured calcium phosphate coating and a possible growth mechanism. *Surface and coatings technology*. **2011**, 205(12), pp.3600-3606.

[41] BRUNNER, Tobias J., BOHNER, Marc, DORA, Claudio, GERBER, Christian and STARK, Wendelin J. Comparison of amorphous TCP nanoparticles to micron-sized alpha-TCP as starting materials for calcium phosphate cements. *Journal of Biomedical Materials Research – Part B: Applied Biomaterials*. **2007,** 83(2), pp. 400-407.

[42] ELIAZ, N. and METOKI, N. Calcium phosphate bioceramics: a review of their history, structure, properties, coating technologies and biomedical applications. *Materials*. **2017**, *10*(4), p.334.

[43] MOURA, Camilla C.G., SOUZA, Maria A., DECHICHI, Paula, ZANETTA-BARBOSA, Darceny, TEIXEIRA, Cristina C. and COELHO, Paulo G. The effect of a nanothickness coating on rough titanium substrate in the osteogenic properties of human bone cells. *Journal of Biomedical Materials Research. Part A*. **2010**, 94A(1), pp. 103-111.

[44] SURMENEV, R. A., SURMENEVA, M. A. and IVANOVA, A. A. Significance of calcium phosphate coatings for the enhancement of new bone osteogenesis–a review. *Acta biomaterialia*. **2014**, 10(2), pp.557-579.

[45] BOSCO, R., EDREIRA, E. R. U., WOLKE, J. G., LEEUWENBURGH, S. C., VAN DEN BEUCKEN, J. J. and JANSEN, J. A. Instructive coatings for biological guidance of bone implants. *Surface and Coatings Technology*. **2013**, 233, pp.91-98.

[46] LAYROLLE, Pierre and DACULSI, Guy. Physicochemistry of Apatite and Its Related Calcium Phosphates. In: LEÓN, B. and JANSEN, J.A. Thin Calcium Phosphate Coatings for

Medical Implants [online]. New York, USA: Springer, 2009, pp. 9-25. ISBN: 9780387777184.

[47] LIU, Q., HUANG, S., MATINLINNA, J. P., CHEN, Z. and PAN, H. Insight into biological apatite: physiochemical properties and preparation approaches. *BioMed research international*, **2013.**

[48] MRÓZ, W., JEDYŃSKI, M., PROKOPIUK, A., ŚLÓSARCZYK, A. and PASZKIEWICZ, Z. Characterization of calcium phosphate coatings doped with Mg, deposited by pulsed laser deposition technique using ArF excimer laser. *Micron*. **2009**, 40(1), pp.140-142.

[49] COTELL, C. M. and GRABOWSKI, K. S. Novel materials applications of pulsed laser deposition. *MRS Bulletin*. **1992**, 17(2), pp.44-53.

[50] GRIGORESCU, S., CARRADÒ, A., ULHAQ, C., FAERBER, J., RISTOSCU, C., DORCIOMAN, G., AXENTE, E., WERCKMANN, J. and MIHAILESCU, I. N. Study of the gradual interface between hydroxyapatite thin films PLD grown onto Ti-controlled sublayers. *Applied Surface Science*. **2007**, 254(4), pp.1150-1154.

[51] DINDA, G. P., SHIN, J. and MAZUMBER, J. Pulsed laser deposition of hydroxyapatite thin films on Ti–6Al–4V: Effect of heat treatment on structure and properties. *Acta biomaterialia*. **2009**, 5(5), pp.1821-1830.

[52] JELÍNEK, M., WEISEROVÁ, M., KOCOUREK, T., ZEZULOVÁ, M. and STRNAD, J. Biomedical properties of laser prepared silver-doped hydroxyapatite. *Laser Physics*. **2011**, 21, pp.1265-1269.

[53] RAU, J. V., SMIRNOV, V. V., LAURETI, S., GENEROSI, A., VARVARO, G., FOSCA, M., FERRO, D., CEASRO, S. N., ALBERTINI, V. R. and BARINOV, S. M. Properties of pulsed laser deposited fluorinated hydroxyapatite films on titanium. *Materials Research Bulletin*. **2010**, 45(9), pp.1304-1310.

[54] GOMES, G. C., BORGH, F. F., OSPINA, R. O., LÓPEZ, E. O., BORGES, F. O. and MELLO, A. Nd: YAG (532 nm) pulsed laser deposition produces crystalline hydroxyapatite thin coatings at room temperature. *Surface and Coatings Technology*. **2017**, 329, pp.174-183.

[55] BOLBASOV, E. N., LAPIN, I. N., SVETLICHNYI, V. A., LENIVTSEVA, Y. D., MALASHICHEVA, A., MALASHICHEV, Y., GOLOVKIN, A. S., ANISSIMOV, Y. G. and TVERDOKHLEBOV, S. I. The formation of calcium phosphate coatings by pulse laser deposition on the surface of polymeric ferroelectric. *Applied Surface Science*. **2015**, 349, pp.420-429.

[56] JEDYNSKI, M., HOFFMAN, J., MROZ, W. and SZYMANSKI, Z. Plasma plume induced during ArF laser ablation of hydroxyapatite. *Applied Surface Science*. **2008**, 255(5), pp.2230-2236.

[57] DUTA, L. and POPESCU, A. C. Current status on pulsed laser deposition of coatings from animal-origin calcium phosphate sources. *Coatings*. **2019**, 9(5), p.335.

[58] VARIOLA, F., BRUNSKI, J. B., ORSINI, G., DE OLIVEIRA, P. T., WAZEN, R. and NANCI, A. Nanoscale surface modifications of medically relevant metals: state-of-the art and perspectives. *Nanoscale*. **2011**, 3(2), pp.335-353.

[59] BOGDANOVICIENE, Irma, BEGANSKIENE, Aldona, TONSUAADU, Kaia, GLASER, Jochen, MEYER, H.-Jurgen and KAREIVA, Aivaras. Calcium hydroxyapatite, $Ca_{10}(PO_4)_6(OH)_2$ ceramics prepared by aqueous sol-gel processing. *Materials Research Bulletin*. **2006**, 41, pp.1754-1762.

[60] ONG, Joo L., YANG, Yunzhi, OH, Sunho, APPLEFORD, Mark, CHEN, Weihui, LIU, Yongeing, KIM, Kyo-Han, PARK, Sangwon, BUMGARDNER, Jeol, HAGGARD, Warren, AGRAWAL, Mauli C., CARNER, David L. and OH, Namsik. Calcium Phosphate Coating Produced by a Sputter Deposition Process. In: Thin Calcium Phosphate Coatings for Medical Implants. LEÓN, Betty and JOHN, Jansen A. USA, New York: Springer, 2009, pp.101-198. ISBN: 9780387777184.

[61] RODRIGUESA, C. V. M., SERRICELLA, P., LINHARES, A. B. R., GUERDES, R. M., BOROJEVIC, R., ROSSI, M. A., DUARTE, M. E. L. and FARINA, M. Characterization of bovine collagen-hydroxyapatite composite scaffold for bone tissue engineering. *Biomaterials.* **2003**, 24, pp.4987-4997.

[62] KUMAR, A., BISWAS, K. and BASU, B. Hydroxyapatite-titanium bulk composites for bone tissue engineering applications. *Journal of Biomedical Materials Research - Part A*. **2015**, 103, pp.791-806.

[63] SIMA, L. E., STAN, G. E., MOROSANU, C. O., MELINESCU, A., LAMCULESCU, A., MELINTE, R., NEAMTU, J. and PETRESCU, S. M. Differentiation of mesenchymal stem cells onto highly adherent radio frequency-sputtered carbonated hydroxylapatite thin films. *Journal of Biomedical Materials Research A.* **2010**, 95A, pp.1203-1214.

[64] KAUR, M. and SINGH, K. Review on titanium and titanium-based alloys as biomaterials for orthopaedic applications. *Materials Science & Engineering C*. **2019**, 102, pp.844-862.

[65] MOHAN, L., DURGALAKSHMI, D., GEETHA, M., SANKARA NARAYANAN, T. S. N. and ASOKAMANI, R. Electrophoretic deposition of nanocomposite (HAp+TiO_2) on titanium alloy for biomedical applications. *Ceramics International*. **2012**, 38(4), pp.3435-3443.

[66] TRUJILLO, Nathan A., FLOREANI, Rachael, MA, Hongyan, BRYERS, James D., WILLIAMS, John D. and POPAT, Ketul C. Antibacterial effects of silver-doped hydroxyapatite thin films sputter deposited on titanium. *Materials Science and Engineering: C*. **2012**, 32(8), pp. 2135-2144.

[67] CHUA, P. H., NEOH, K. G., SHI, Z. and KANG, E. T. Structural stability and bioapplicability assessment of hyaluronic acid–chitosan polyelectrolyte multilayers on titanium substrates. *Journal of Biomedical Materials Research Part A*. **2008**, 87(4), pp.1061-1074.

[68] CLERIES, L., FERNANDEZ-PRADAS, J. M., SARDIN, G. and MORENZA, J. L. Dissolution behaviour of calcium phosphate coatings obtained by laser ablation. *Biomaterials*. **1998**, 19, pp.1483-1487.

[69] ZHANGZ, E. L. and ZOU, C. M. Porous titanium and silicon-substituted hydroxyapatite biomodification prepared by a biomimetic process: Characterization and in vivo evaluation. *Actabiomaterialia*. **2009**, 5, pp.1732-1741.

[70] CAMAIONI, A., CACCIOTTI, I., CAMPAGNOLO, L. and BIANCO, A. Silicon substituted hydroxyapatite for biomedical applications. In: MUCALO, M, ed. Hydroxyapatite for Biomedical Applications. United Kingdom: Elsevier Ltd, **2015**, Chapter 15, pp.343-373.

[71] PIETAK, Alexis M., REID, Joel W., STOTT, Malcom J. and SAYER, Michael. Silicon substitution in the calcium phosphate bioceramics. *Biomaterials.* **2007**, 28(28), pp.4023-4032.

[72] SOLLA, E. L., BORRAJO, J. P., GONZÁLEZ, P., SERRA, J., CHIUSSI, S., LEÓN, B. and GARCÍA LÓPEZ, J. Study of the composition transfer in the pulsed laser deposition of silicon substituted hydroxyapatite thin films. *Applied Surface Science*. **2007**, 253(19), pp.8282-8286.

[73] SOLLA, E. L., GONZÁLEZ, P., SERRA, J., CHIUSSI, S., LEÓN, B. and GARCÍA LÓPEZ, J. Pulsed laser deposition of silicon substituted hydroxyapatite coatings from synthetical and biological sources. *Applied Surface Science*. **2007**, 254(4), pp.1189-1193.

[74] PREDOI, Daniela, ICONARU, Simona L. and PREDOI, Mihai V. Fabrication of silver-and zinc-doped hydroxyapatite coatings for enhancing antimicrobial effect. *Coatings*. **2020**, 10(9), p.905.

[75] HOOVER, Sean, TARAFDER, Solaiman, BANDYOPADHYAY, Amit and BOSE, Susmita. Silver doped resorbable tricalcium phosphate scaffolds for bone graft applications. *Materials Science and Engineering: C*. **2017**, 79, pp.763-769.

[76] RIBEIRO, M., FERRAZ, M. P., MONTEIRO, F. J., FERNANDES, M. H., BEPPU, M. M., MANTIONE, D. and SARDON, H. Antibacterial silk fibroin/nanohydroxyapatite hydrogels with silver and gold nanoparticles for bone regeneration. *Nanomedicine: Nanotechnology, Biology and Medicine*. **2017**, 13(1), pp.231-239.

[77] KE, Dongxu, VU, Ashley A., BANDYOPADHYAY, Amit and BOSE, Susmita. Compositionally graded doped hydroxyapatite coating on titanium using laser and plasma spray deposition for bone implants. *Acta biomaterialia*. **2019**, 84, pp.414-423.

[78] RAU, Julietta V., CACCIOTTI, Ilaria, LAURETI, Sara, FOSCA, Marco, VARVARO, Gaspare and LATINI, Alessandro. Bioactive, nanostructured Si-substituted hydroxyapatite coatings on titanium prepared by pulsed laser deposition. *Journal of Biomedical Materials Research Part B: Applied Biomaterials*. **2015**, 103(8), pp.1621-1631.

[79] ROY, Mangal, FIELDING, Gary A., BEYENAL, Haluk, BANDYOPADHYAY, Amit and BOSE, Susmita. Mechanical, in vitro antimicrobial, and biological properties of plasma-sprayed silver-doped hydroxyapatite coating. *ACS applied materials & interfaces*. **2012**, 4(3), pp.1341-1349.

[80] ICONARU, Simona L., PREDOI, Daniela, CIOBANU, Carmen S., MOTELICA-HEINO, Mikael, GUEGAN, Régis and BLEOTU, Coralia. Development of Silver Doped Hydroxyapatite Thin Films for Biomedical Applications. *Coatings*. **2022**, 12(3), 341.

[81] ERAKOVIĆ, S., JANKOVIĆ, A., RISTOSCU, C., DUTA, L., SERBAN, N., VISAN, A., MICHALESCU, I. N., STAN, G. E., SOCOL, M., IORDACHE, O. and DUMITRESCU, I. Antifungal activity of Ag: hydroxyapatite thin films synthesized by pulsed laser deposition on Ti and Ti modified by TiO2 nanotubes substrates. *Applied Surface Science*. **2014**, 293, pp.37-45.

[82] YOUNG-AH, Yi, YOUNG-BUM, Park, HYUNMIN, Choi, KEUN-WOO, Lee, SUN-JAI, Kim, KWANG-MAHN, Kim, SEUNGHAN, Oh and JUNE-SUNG, Shim. The Evaluation of Osseointegration of Dental Implant Surface with Different Size of TiO2 Nanotube in Rats. *Journal of nanomaterials*. **2015.**

[83] CAI, Y. L., ZHANG, J. J., ZHANG, S., VENKATRAMAN, S. S., ZENG, X. T., DU, H. J. and MONDAL, D. Osteoblastic cell response on fluoridated hydroxyapatite coatings: The effect of magnesium incorporation. *Biomedical Materials*. **2010**, 5, p. 054114.

[84] LANDI, Elena, LOGROSCINO, Logroscino, PROIETTI, Luca, TAMPIERI, Anna, SANDRI, Monica and SPRIO, Simone. Biomimetic Mg-substituted hydroxyapatite: From synthesis to invivo behavior. *Journal of Materials Science: Materials in Medicine*. **2008**, 19, pp.239-247.

[85] MRÓZ, Waldemar, BUDNER, Bogusław, SYROKA, Renata, NIEDZIELSKI, Kryspin, GOLAŃSKI, Grzegorz, SlÓSARCZYK, Anna, SCHWARZE, Dieter and DOUGLAS, Timothy E. L. In vivo implantation of porous titanium alloy implants coatedwith magnesium-doped octacalcium phosphate and hydroxyapatitethin films using pulsed laser deposition. *Journal of Biomedical Materials Research Part B: Applied Biomaterials.* **2015**, 103(1), pp.1-241.

[86] NIINOMI, Mitsuo. Mechanical biocompatibilities of titanium alloys for biomedical applications. *Journal of the Mechanical Behavior of Biomedical Materials*. **2008**, 1(1), pp.30-42.

[87] SEAL, B. L., OTERO, T. C. and PANITCH, A. Polymeric biomaterials for tissue and organ regeneration. *Materials Science and Engineering: R: Reports*. **2001**, 34(4-5), pp,147-230.

[88] CUI, Z., DRIOLI, E. and LEE, Y. M. Recent progress in fluoropolymers for membranes. *Progress in Polymer Science*. **2014**, 39(1), pp.164-198.

[89] KOCHERVINSKII, V. V. The structure and properties of block poly (vinylidene fluoride) and systems based on it. *Russian chemical reviews*. **1996**, 65(10), p.865.

[90] DAMARAJU, S. M., WU, S., JAFFE, M. and ARINZEH, T. L. Structural changes in PVDF fibers due to electrospinning and its effect on biological function. *Biomedical Materials*. **2013,** 8(4), p.045007.

[91] RIBEIRO, C., PÄRSSINEN, J., SENCADAS, V., CORREIA, V., MIETTINEN, S., HYTÖNEN, V. P. and LANCEROS-MÉNDEZ, S. Dynamic piezoelectric stimulation enhances osteogenic differentiation of human adipose stem cells. *Journal of Biomedical Materials Research Part A*. **2015,** 103(6), pp.2172-2175.

[92] MARINO, A. A., ROSSON, J., GONZALEZ, E., JONES, L., ROGERS, S. and FUKADA, E. Quasi-static charge interactions in bone. *Journal of Electrostatics*. **1988**, 21(2-3), pp.347-360.

[93] JIN, G., YAO, Q., ZHANG, S. and ZHANG, L. Surface modifying of microporous PTFE capillary for bilirubin removing from human plasma and its blood compatibility. *Materials Science and Engineering: C*. **2008**, 28(8), pp.1480-1488.

[94] YOUNG, T. H., CHANG, H. H., LIN, D. J. and CHENG, L. P. Surface modification of microporous PVDF membranes for neuron culture. *Journal of Membrane Science*. **2010**, 350(1-2), pp.32-41.

[95] SHTANSKY, D. V., GRIGORYAN, A. S., TOPORKOVA, A. K., ARKHIPOV, A. V., SHEVEYKO, A. N. and KIRYUKHANTSEV-KORNEEV, P. V. Modification of polytetrafluoroethylene implants by depositing TiCaPCON films with and without stem cells. *Surface and Coatings Technology*. **2011**, 206(6), pp.1188-1195.

[96] ESHTIAGH-HOSSEINI, H., HOUSSAINDOKHT, M. R., CHAHKANDHI, M. and YOUSSEFI, A. Preparation of anhydrous dicalcium phosphate, DCPA, through sol-gel process, identification and phase transformation evaluation. *Journal of Non-Crystalline Solids*. **2008**, 354(32), pp.3854-3857.

[97] MONTAZEROLGHAEM, M., OTT, M. K., ENGQVIST, H., MELHUS, H. and RASMUSSON, A. J. Resorption of monetite calcium phosphate cement by mouse bone marrow derived osteoclasts. *Materials Science and Engineering: C*. **2015**, 52, pp.212-218.

[98] TAMIMI, F., LE NIHOUANNEN, D., EIMAR, H., SHEIKH, Z., KOMAROVA, S. and BARRALET, J. The effect of autoclaving on the physical and biological properties of dicalcium phosphate dihydrate bioceramics: Brushite vs. monetite. *Acta biomaterialia*. **2012**, 8(8), pp.3161-3169.

[99] ORYAN, A., ALIDADI, S. and BIGHAM-SADEGH, A. Dicalcium phosphate anhydrous: An appropriate bioceramic in regeneration of critical-sized radial bone defects in rats. *Calcified tissue international*. **2017**, 101, pp.530-544.

[100] WITTE, F., FEYERABEND, F., MAIER, P., FISCHER, J., STÖRMER, M., BLAWERT, C., DIETZEL, W. and HORT, N. Biodegradable magnesium–hydroxyapatite metal matrix composites. *Biomaterials*. **2007**, 28(13), pp.2163-2174.

[101] WITTE, F., ULRICH, H., RUDERT, M. and WILLBOLD, E. Biodegradable magnesium scaffolds: Part I: appropriate inflammatory response. *Journal of biomedical materials research Part A*. **2007**, 81(3), pp.748-756.

[102] WITTE, F., ULRICH, H., PALM, C. and WILLBOLD, E. Biodegradable magnesium scaffolds: Part II: Peri-implant bone remodeling. *Journal of biomedical materials research Part A*. **2007**, 81(3), pp.757-765.

[103] LI, N. and ZHENG, Y. Novel magnesium alloys developed for biomedical application: a review. *Journal of Materials Science & Technology*. **2013**, 29(6), pp.489-502.

[104] WITTE, F. The history of biodegradable magnesium implants: a review. *Acta biomaterialia*. **2010**, 6(5), pp.1680-1692.

[105] QIAO, Z., SHI, Z., HORT, N., ABIDIN, N. I. Z. and ATRENS, A. Corrosion behaviour of a nominally high purity Mg ingot produced by permanent mould direct chill casting. *Corrosion Science*. **2012**, 61, pp.185-207.

[106] SONG, G. Control of biodegradation of biocompatable magnesium alloys. *Corrosion science*. **2007**, 49(4), pp.1696-1701.

[107] RAU, J. V., ANTONIAC, I., FOSCA, M., DE BONIS, A., BLAJAN, A. I., COTRUT, C., GRAZIANI, V., CURCIO, M., CRICENTI, A., NICULESCU, M. and ORTENZI, M. Glass-ceramic coated Mg-Ca alloys for biomedical implant applications. *Materials Science and Engineering: C*. **2016**, 64, pp.362-369.

[108] SINGH, R. K., SRIVASTAVA, M., PRASAD, N. K., AWASTHI, S., DHAYALAN, A. and KANNAN, S. Iron doped β-Tricalcium phosphate: Synthesis, characterization, hyperthermia effect, biocompatibility and mechanical evaluation. *Materials Science and Engineering: C*. **2017**, 78, pp.715-726.

[109] ANTONIAC, I. V., FILIPESCU, M., BARBARO, K., BONCIU, A., BIRJEGA, R., COTRUT, C. M., GALVANO, E., FOSCA, M., FADEEVA, I. V., VADALÀ, G. and DINESCU, M. Iron ion-doped tricalcium phosphate coatings improve the properties of biodegradable magnesium alloys for biomedical implant application. *Advanced Materials Interfaces*. **2020**, 7(16), p.2000531.

[110] LI, Z., GU, X., LOU, S. and ZHENG, Y. The development of binary Mg–Ca alloys for use as biodegradable materials within bone. *Biomaterials*. **2008**, 29(10), pp.1329-1344.

[111] SERRE, C. M., PAPILLARD, M., CHAVASSIEUX, P., VOEGEL, J. C. and BOIVIN, G. Influence of magnesium substitution on a collagen–apatite biomaterial on the production of a calcifying matrix by human osteoblasts. *Journal of Biomedical Materials Research*. **1998**, 42(4), pp.626-633.

[112] XIE, L., YANG, Y., FU, Z., LI, Y., SHI, J., MA, D., LIU, S. and LUO, D. Fe/Zn-modified tricalcium phosphate (TCP) biomaterials: Preparation and biological properties. *RSC advances*. **2019**, 9(2), pp.781-789.

[113] SMIRNOV, I. V., RAU, J. V., FOSCA, M., DE BONIS, A., LATINI, A., TEGHIL, R., KALITA, V. I., FEDOTOV, A. Y., GUDKOV, S. V., BARANCHIKOV, A. E. and KOMLEV, V. S. Structural modification of titanium surface by octacalcium phosphate via Pulsed Laser Deposition and chemical treatment. *Bioactive Materials*. **2017**, 2(2), pp.101-107.

[114] KOMLEV, V. S., BARINOV, S. M., BOZO, I. I., DEEV, R. V., EREMIN, I. I., FEDOTOV, A. Y., GURIN, A. N., KHROMOVA, N. V., KOPNIN, P. B., KUVSHINOVA, E. A. and MAMONOV, V. E. Bioceramics composed of octacalcium phosphate demonstrate enhanced biological behavior. *ACS applied materials & interfaces*. **2014**, 6(19), pp.16610-16620.

[115] SUZUKI, O., NAKAMURA, M., MIYASAKA, Y., KAGAYAMA, M. and SAKURAI, M. Bone Formation on Synthetic Precursors of Hydroxyapatite. *The Tohoku Journal of Experimental Medicine*. **1991**, 164(1), pp.37-50.

[116] BIGI, A., BRACCI, B., CUISINIER, F., ELKAIM, R., FINI, M., MAYER, I., MIHAILESCU, I. N., SOCOL, G., STURBA L. and TORRICELLI, P. Human osteoblast response to pulsed laser deposited calcium phosphate coatings. *Biomaterials*. **2005**, 26(15), pp.2381-2389.

[117] DEKKER, R. J., DE BRUIJN, J. D., STIGTER, M., BARRERE, F., LAYROLLE, P., VAN BLITTERSWIJK, C. A. Bone tissue engineering on amorphous carbonated apatite and crystalline octacalcium phosphate-coated titanium discs. *Biomaterials*. **2005**, 26(25), pp.5231-5239.

[118] SUZUKI, Osamu, KAMAKURA, Shinji, KATAGIRI, Takenobu, NAKAMURA, Masanori, ZHAO, Baohong, HONDA, Yoshitomo and KAMIJO, Ryutaro. Bone formation enhanced by implanted octacalcium phosphate involving conversion into Ca-deficient hydroxyapatite. *Biomaterials*. **2006**, 27(13), pp.2671-2681.

[119] SUZUKI, O., KAMAKURA, S. and KATAGIRI, T.. Surface chemistry and biological responses to synthetic octacalcium phosphate. *Journal of biomedical materials research. Part B, Applied biomaterials*. **2006**, 77B(1), pp.201-212.

[120] MIYATAKE, N., KISHIMOTO, K. N., ANADA, T., IMAIZUMI, H., ITOI, E. and SUZUKI, O. Effect of partial hydrolysis of octacalcium phosphate on its osteoconductive characteristics. *Biomaterials*. **2009**, 30(6), pp.1005-1014.

[121] LIU, Y., COOPER, P. R., BARRALET, J. E. and SHELTON, R. M. Influence of calcium phosphate crystal assemblies on the proliferation and osteogenic gene expression of rat bone marrow stromal cells. *Biomaterials*. **2007**, 28(7), pp.1393-1403.

[122] MRÓZ, W., BOMBALSKA, A., BUDNER, B., BURDYŃSKA, S., JEDYŃSKI, M., PROKOPIUK, A., MENASZEK, E., ŚCISŁOWSKA-CZARNECKA, A., NIEDZIELSKA,

A. and NIEDZIELSKI, K. Comparative study of hydroxyapatite and octacalcium phosphate coatings deposited on metallic implants by PLD method. *Applied Physics A*. **2010**, 101, pp.713-716.

[123] DEWIDAR, M. M., KHALIL, K. A. and LIM, J. K. Processing and mechanical properties of porous 316L stainless steel for biomedical applications. *Transactions of Nonferrous Metals Society of China*. **2007**, 17(3), pp.468-473.

[124] BAINO, F., NOVAJRA, G., MIGUEZ-PACHECO, V., BOCCACCINI, A. R. and VITALE-BROVARONE, C. Bioactive glasses: Special applications outside the skeletal system. *Journal of Non-Crystalline Solids*. **2016**, 432A, pp.15-30.

[125] JONES, J. R. Review of bioactive glass: from Hench to hybrids. *Acta Biomater*. **2013**, 9(1), pp.4457-4486.

[126] HENCH, L. L. The story of Bioglass. *Journal of materials science. Materials in medicine*. **2006**, 17(11), pp.967-978.

[127] HENCH, L. L., Splinter, R.J., Allen, W.V., Greenlee, T.K. Bonding mechanisms at the interface of ceramic prosthetic materials. *Journal of Biomedical Materials Research.* **1971**, 5(6), pp.117-141.

[128] HUPA, Leena, WANG, Xiaoju and EQTESADI, Siamak. Bioactive glasses. In: MUSGRAVES, David J., HU, Juejun and CALVEZ, Laurent. Springer Handbook of Glass [online]. Cham, Switzerland: 2019, pp.813-842.

[129] RAHAMAN, M. N., DAY, D. E., BAL, B. S., FU, Q., JUNG, S. B., BONEWALD, L. F. and TOMSIA, A. P. Bioactive glass in tissue engineering. *Acta Biomater*. **2011**, 7(6), pp.2355-2373.

[130] HENCH, Larry L. Bioceramics. *Journal of the American Ceramic Society.* **1998**, 81(7), pp. 1705-1728.

[131] DHINASEKARAN, D., KALIARAJ, G. S., JAGANNATHAN, M., RAJENDRAN, A. R., PRAKASARAO, A., GANESAN, S., SUBRAMANIAN, B. Pulsed laser deposition of nanostructured bioactive glass and hydroxyapatite coatings: Microstructural and electrochemical characterization. *Materials Science and Engineering: C*. **2021**, 130, p.112459.

[132] TEGHIL, R., CURCIO, M. and DE BONIS, A. Substituted hydroxyapatite, glass, and glass-ceramic thin films deposited by nanosecond pulsed laser deposition (PLD) for biomedical applications: A systematic review. *Coatings*. **2021**, 11(7), p.811.

[133] KAUR, Gurbinder, PANDEY, Om P., SINGH, Kulvir, HOMA, Dan, SCOTT, Brian and PICKRELL, Gary. A review of bioactive glasses: their structure, properties, fabrication and apatite formation. *Journal of Biomedical Materials Research Part A.* **2014**, 102(1), pp.254-274.

[134] NARAYANAN, R., SESHADRI, S. K., KWON, T. Y. and KIM, K. H. Calcium phosphate-based coatings on titanium and its alloys. *Journal of biomedical materials research. Part B, Applied biomaterials.* **2008**, 85(1), pp.279-299.

[135] ZHAO, Y., SONG, M. and LIU, J. Characteristics of bioactive glass coatings obtained by pulsed laser deposition. *Surface and Interface Analysis: An International Journal devoted to the development and application of techniques for the analysis of surfaces, interfaces and thin films*. **2008**, 40(11), pp.1463-1468.

[136] WANG, H., ZHAO, S., ZHOU, J., SHEN, Y., HUANG, W., ZHANG, C., RAHAMAN, M. N. and WANG, D. Evaluation of borate bioactive glass scaffolds as a controlled delivery system for copper ions in stimulating osteogenesis and angiogenesis in bone healing. *Journal of Materials Chemistry B*. **2014**, 2(48), pp.8547-8557.

[137] HOPPE, A., GÜLDAL, N. S. and BOCCACCINI, A. R. A review of the biological response to ionic dissolution products from bioactive glasses and glass-ceramics. *Biomaterials*. **2011**, 32(11), pp.2757-2774.

[138] STOJANOVIC, D., JOKIC, B., VELJOVIC, D., PETROVIC, R., USKOKOVIC, P.S. and JANACKOVIC, D. Bioactive glass–apatite composite coating for titanium implant synthesized by electrophoretic deposition. *Journal of the European Ceramic Society*. **2007**, 27(2-3), pp.1595-1599.

[139] KWIATKOWSKA, J., SUCHANEK, K. and RAJCHEL, B. Bioactive glass coatings synthesized by pulsed laser deposition technique. *Acta Physica Polonica A*. **2012**, 121(2), pp.502-505.

[140] SANZ, C. K., DOS SANTOS, A. R., DA SILVA, M. H. P., MARCAL, R., TUTE, E. M., MEZA, E. L., MELLO, A., BORGHI, F. F. and DE SOUZA CAMARGO JR., S. A. Niobo-phosphate bioactive glass films produced by pulsed laser deposition on titanium surfaces for improved cell adhesion. *Ceramics International*. **2019**, 45(14), pp.18052-18058.

[141] DENRY, I. L., HOLLOWAY, J. A., NAKKULA, R. J. and WALTERS, J. D. Effect of niobium content on the microstructure and thermal properties of fluorapatite glass-ceramics. *Journal of Biomedical Materials Research.Part B, Applied Biomaterials*. **2005**, 75(1), pp.18-24.

[142] DE SOUZA, U. P .L., LOPES, J. H., FERREIRA, F. V., MARTIN, R. A., BERTRAN, C. A. and CAMILLI, J.A. Evaluation of effectiveness of 45S5 bioglass doped with niobium for repairing critical-sized bone defect in in vitro and in vivo models. *Journal of Biomedical Materials Research Part A*. **2020**, 108(3), pp.446-457.

[143] BONETTI, L., ALTOMARE, L., BONO, N., PANNO, E., CAMPIGLIO, C. E., DRAGHI, L., CANDIANI, G., FARÈ, S., BOCCACCINI, A. R. and DE NARDO, L. Electrophoretic processing of chitosan based composite scaffolds with Nb-doped bioactive glass for bone tissue regeneration. *Journal of Materials Science: Materials in Medicine*. **2020**, 31, pp.1-12.

[144] KRAJEWSKI, A., MALAVOLTI, R. and PIANCASTELLI, A. Albumin adhesion on some biological and non-biological glasses and connection with their Z-potentials. *Biomaterials.* **1996**, 17(1), pp.53-60.

[145] TORRICELLI, P., FINI, M., GIAVARESI, G., ROCCA, M., PIERINI, G. and GIARDINO, R. Isolation and characterization of osteoblast cultures from normal and osteopenic sheep for biomaterials evaluation. *Journal of biomedical materials research*. **2000**, 52(1), pp.177-182.

[146] FINI, M., GIAVARESI, G., TORRICELLI, P., KRAJEWSKI, A., RAVAGLIOLI, A., BELMONTE, M. M., BIAGINI, G. and GIARDINO, R. Biocompatibility and osseointegration in osteoporotic bone. *The Journal of bone and joint surgery. British volume.* **2001**, 83(1), pp.139-143.

[147] LI, J., ZHAI, D., LV, F., YU, Q., MA, H., YIN, J., YI, Z., LIU, M., CHANG, J. and WU, C. Preparation of copper-containing bioactive glass/eggshell membrane nanocomposites for improving angiogenesis, antibacterial activity and wound healing. *Acta biomaterialia*. **2016**, 36, pp.254-266.

[148] WU, C., ZHOU, Y., XU, M., HAN, P., CHEN, L., CHANG, J. and XIAO, Y. Copper-containing mesoporous bioactive glass scaffolds with multifunctional properties of angiogenesis capacity, osteostimulation and antibacterial activity. *Biomaterials*. **2013**, 34(2), pp.422-433.

[149] JAISWAL, S., MCHALE, P. and DUFFY, B. Preparation and rapid analysis of antibacterial silver, copper and zinc doped sol-gel surfaces. *Colloids and Surfaces B: Biointerfaces*. **2012**, 94, pp.170-176.

[150] MIGUEZ-PACHECO, V., HENCH, L. L. and BOCCACCINI, A. R. Bioactive glasses beyond bone and teeth: Emerging applications in contact with soft tissues. *Acta biomaterialia*. **2015**, 13, pp.1-15.

[151] XU, H., LV, F., ZHANG, Y., YI, Z., KE, Q., WU, C., LIU, M. and CHANG, J. Hierarchically micro-patterned nanofibrous scaffolds with a nanosized bio-glass surface for accelerating wound healing. *Nanoscale*. **2015**, 7(44), pp.18446-18452.

[152] DEVI, P. S., BANERJEE, S., CHOWDHURY, S. R. and KUMAR, G. S. Eggshell membrane: a natural biotemplate to synthesize fluorescent gold nanoparticles. *RSC advances*. **2012**, 2(30), pp.11578-11585.

[153] BALÁŽ, M. Eggshell membrane biomaterial as a platform for applications in materials science. *Acta biomaterialia*. **2014**, 10(9), pp.3827-3843.

[154] CAI, H., LIANG, P., HÜBNER, R., ZHOU, S., LI, Y., SUN, J., XU, N. and WU, J. Composition and bandgap control of Al x Ga 1− x N films synthesized by plasma-assisted pulsed laser deposition. *Journal of Materials Chemistry C*. **2015**, 3(20), pp.5307-5315.

[155] ZHANG, F. B., SAITO, K., TANAKA, T., NISHIO, M. and GUO, Q. X. Structural and optical properties of Ga2O3 films on sapphire substrates by pulsed laser deposition. *Journal of Crystal Growth*. **2014**, 387, pp.96-100.

[156] KOCOUREK, T., JELINEK, M., VORLÍČEK, V., ZEMEK, J., JANČA, T., ŽÍŽKOVÁ, V., PODLAHA, J. and POPOV, C. DLC coating of textile blood vessels using PLD. *Applied Physics A*. **2008**, *93*, pp.627-632.

[157] NARAYAN, R. J. Diamond-like carbon: Medical and mechanical applications. In: EASON, Robert, ed. Pulsed Laser Deposition of Thin Films [online]. Hoboken, NJ, USA: John Wiley & Sons, Inc., 2007, pp.333-355. ISBN 9780470052129.

[158] STOCK, F., ANTONI, F., AUBEL, D., HAJJAR-GARREAU, S. and MULLER, D. Pure carbon conductive transparent electrodes synthetized by a full laser deposition and annealing process. *Applied Surface Science*. **2020**, *505*, p.144505.

[159] HAUERT, R., THORWARTH, K. and THORWARTH, G. An overview on diamond-like carbon coatings in medical applications. *Surface and Coatings Technology*. **2013**, *233*, pp.119-130.

[160] MIKSOVSKY, J., VOSS, A., KOZAROVA, R., KOCOUREK, T., PISARIK, P., CECCONE, G., KULISCH, W., JELINEK, M., APOSTOLOVA, M. D., REITHMAIER, J. P. and POPOV, C. Cell adhesion and growth on ultrananocrystalline diamond and diamond-like carbon films after different surface modifications. *Applied surface science*. **2014**, 297, pp.95-102.

[161] SALGUEIREDO, E., VILA, M., SILVA, M. A., LOPES, M. A., SANTOS, J. D., COSTA, F. M., SILVA, R. F., GOMES, P. S. and FERNANDES, M. H. Biocompatibility evaluation of DLC-coated Si3N4 substrates for biomedical applications. *Diamond and related Materials*. **2008**, 17(4-5), pp.878-881.

[162] MOCHIZUKI, A., OGAWA, T., OKAMOTO, K., NAKATANI, T. and NITTA, Y. Blood compatibility of gas plasma-treated diamond-like carbon surface—Effect of physicochemical properties of DLC surface on blood compatibility. *Materials Science and Engineering: C*. **2011**, 31(3), pp.567-573.

[163] AZZI, M., AMIRAULT, P., PAQUETTE, M., KLEMBERG-SAPIEHA, J. E. and MARTINU, L. Corrosion performance and mechanical stability of 316L/DLC coating system: Role of interlayers. *Surface and Coatings Technology*. **2010**, 204(24), pp.3986-3994.

[164] BATORY, D., SZYMAŃSKI, W. and CŁAPA, M. Mechanical and tribological properties of gradient aC: H/Ti coatings. *Materials Science-Poland*. **2013**, 31, pp.415-423.

[165] BATORY, D., BLASZCZYK, T., CLAPA, M. and MITURA, S. Investigation of anti-corrosion properties of Ti: C gradient layers manufactured in hybrid deposition system. *Journal of Materials Science*. **2008**, 43, pp.3385-3391.

[166] BOCIAGA, D. and MITURA, K. Biomedical effect of tissue contact with metallic material used for body piercing modified by DLC coatings. *Diamond and related materials*. **2008**, 17(7-10), pp.1410-1415.

[167] ROTHAMMER, B., MARIAN, M., NEUSSER, K., BARTZ, M., BÖHM, T., KRAUß, S., SCHROEDER, S., UHLER, M., THIELE, S., MERLE, B. and KRETZER, J. P. Amorphous carbon coatings for total knee replacements—Part II: tribological behavior. *Polymers*. **2021**, 13(11), p.1880.

[168] MILAN, P. B., KHAMSEH, S., ZARRINTAJ, P., RAMEZANZADEH, B., BADAWI, M., MORISSET, S., VAHABI, H., SAEB, M .R. and MOZAFARI, M. Copper-enriched diamond-like carbon coatings promote regeneration at the bone-implant interface. *Heliyon*. **2020**, 6(4), p.e03798.

[169] LIU, C., ZHAO, Q., LIU, Y., WANG, S. and ABEL, E. W. Reduction of bacterial adhesion on modified DLC coatings. *Colloids and Surfaces B: Biointerfaces*. **2008**, 61(2), pp.182-187.

[170] OHGOE, Yasuharu, TAKADA, Satoshi, HIRAKURI, Kenji K., TSUCHIMOTO, Katsuya, HOMMA, Akihiko, MIYAMATSU, Toshinobu, SAITOU, Tomoyuki, FRIEDBACHER, Gernot, TATSUMI, Eisuke, TAENAKA, Yoshiyuki and FUKUI, Yasuhiro. Investigating the Functionality of Diamond-Like Carbon Films on an Artificial Heart Diaphragm. *ASAIO Journal*. **2003**, 49(6), pp.701-707.

[171] NAKAGAWA, T., OHISHI, R., OHTAKE, N., TAKAI, O., TSUTSUI, N., TSUTSUI, Y., MURAKI, Y. and OGURA, J. Segment-structured diamond-like carbon coatings on polymer catheter. *Journal of Solid Mechanics and Materials Engineering*. **2009**, 3(2), pp.358-365.

[172] LAUBE, N. C., BRADENAHL, J., SCHMIDT, M. E., MEISSNER, A., KLEINEN, L. and MUELLER, S. C. 1096: Diamond-Like Carbon Coatings Reduce the Extent of Encrustation of Indwelling Catheter Surfaces and Ureteral Stents. *The Journal of Urology.* **2005**, 173(4S), pp.297-297.

[173] SAITO, K., HIRATUKA, M., MANOME, Y., FUJIOKA, K., OHGOE, Y., HONDA, H. and HIRAKURI, K. Effects of zinc-containing diamond-like carbon coated splints on the healing of fractures in mice: A pilot study. *Diamond and Related Materials*. **2021**, 119, p.108574.

[174] LU, Y., HUANG, G., WANG, S., MI, C., WEI, S., TIAN, F., LI, W., CAO, H. and CHENG, Y. A review on diamond-like carbon films grown by pulsed laser deposition. *Applied Surface Science*. **2021**, 541, p.148573.

[175] OSKOMOV, K. V. and VIZIR, A. V. Investigation of plasma ion composition generated by high-power impulse magnetron sputtering (HiPIMS) of graphite. *Journal of Physics: Conference Series*. **2019**, 1393(1), p. 012018.

[176] GUPTA, S., SACHAN, R. and NARAYAN, J. Scale-up of Q-carbon and nanodiamonds by pulsed laser annealing. *Diamond and Related Materials*. **2019**, 99, p.107531.

[177] ERDEMIR, A. and MARTIN, J. M. Superior wear resistance of diamond and DLC coatings. *Current Opinion in Solid State and Materials Science*. **2018**, 22(6), pp.243-254.

[178] BEWILOGUA, K. and HOFMANN, D. History of diamond-like carbon films — From first experiments to worldwide applications. *Surface and Coatings Technology*. **2014**, 242, pp.214-225.

[179] PANDA, M., KRISHNAN, R., MADAPU, K. K., PANDA, P., SAHOO, M., RAMASESHAN, R., SUNDARI, T. and KAMRUDDIN, M. Influence of particulate on surface energy and mechanical property of diamond-like carbon films synthesized by pulsed laser deposition. *Applied Surface Science*. **2019**, 484, pp.1176-1183.

[180] ZOUBOS, H., KOUTSOKERAS, L. E., ANAGNOSTOPOULOS, D. F., LIDORIKIS, E., KALOGIROU, S. A., WILDES, A. R., KELIRES, P. C. and PATSALAS, P. Broadband optical absorption of amorphous carbon/Ag nanocomposite films and its potential for solar harvesting applications. *Solar energy materials and solar cells*. **2013**, 117, pp.350-356.

[181] FOONG, Y. M., KOH, A. T. T., LIM, S. R., HSIEH, J. and CHUA, D. H. C. Materials properties of ZnO/diamond-like carbon (DLC) nanocomposite fabricated with different source of targets. *Diamond and related materials*. **2012**, 25, pp.103-110.

[182] MENEGAZZO, N., JIN, C., NARAYAN, R. J. and MIZAIKOFF, B. Compositional and Electrochemical Characterization of Noble Metal− Diamondlike Carbon Nanocomposite Thin Films. *Langmuir*. **2007**, *23*(12), pp.6812-6818.

[183] PANDA, M., KRISHNAN, R., KRISHNA, N. G., AMIRTHAPANDIAN, S., MAGUDAPATHY, P. and KAMRUDDIN, M. Tuning the tribological property of PLD deposited DLC-Au nanocomposite thin films. *Ceramics International*. **2019**, 45(7), pp.8847-8855.

[184] GRIGORIEV, S. N., FOMINSKI, V. Y., ROMANOV, R. I., VOLOSOVA, M. A. and SHELYAKOV, A. V. Effect of energy fluence and Ti/W co-deposition on the structural, mechanical and tribological characteristics of diamond-like carbon coatings obtained by pulsed Nd: YAG laser deposition on a steel substrate. *Surface and Coatings Technology*. **2014**, 259, pp.415-425.

[185] NEUVILLE, S. New application perspective for tetrahedral amorphous carbon coatings. *QScience Connect*. **2014**, 2014(1), p.8.

[186] STOCK, F., ANTONI, F., LE NORMAND, F., MULLER, D., ABDESSELAM, M., BOUBICHE, N. and KOMISSAROV, I. High performance diamond-like carbon layers obtained by pulsed laser deposition for conductive electrode applications. *Applied Physics A*. **2017**, 123, pp.1-5.

[187] GUPTA, S., BHAUMIK, A., SACHAN, R. and NARAYAN, J. Structural evolution of Q-carbon and nanodiamonds. *Jom*. **2018**, 70, pp.450-455.

[188] KUMAR, I. and KHARE, A. Optical nonlinearity in nanostructured carbon thin films fabricated by pulsed laser deposition technique. *Thin Solid Films*. **2016**, 611, pp.56-61.

[189] MADDI, C., DONNET, C., LOIR, A. S., TITE, T., BARNIER, V., ROJAS, T. C., SANCHEZ-LOPEZ, J. C., WOLSKI, K. and GARRELIE, F. High N-content aC: N films elaborated by femtosecond PLD with plasma assistance. *Applied Surface Science*. **2015**, 332, pp.346-353.

[190] BOURQUARD, F., TITE, T., LOIR, A. S., DONNET, C. and GARRELIE, F. Control of the graphite femtosecond ablation plume kinetics by temporal laser pulse shaping: Effects on pulsed laser deposition of diamond-like carbon. *The Journal of Physical Chemistry C*. **2014**, 118(8), pp.4377-4385.

[191] FLORES-RUIZ, F. J., HERRERA-GOMEZ, A., CAMPS, E. and ESPINOZA-BELTRÁN, F.J. Elastic heterogeneities at the nanoscale in DLC films grown by PLD. *Materials Research Express*. **2015**, 2(2), p.025009.

[192] GUZMÁN, F., FAVRE, M., RUIZ, H. M., HEVIA, S., CABALLERO, L. S., WYNDHAM, E. S., BHUYAN, H., FLORES, M. and MÄNDL, S. Pulsed laser deposition of thin carbon films in a neutral gas background. *Journal of Physics D: Applied Physics*. **2013**, 46(21), p.215202.

[193] BOURQUARD, F., MADDI, C., DONNET, C., LOIR, A. S., BARNIER, V., WOLSKI, K. and GARRELIE, F. Effect of nitrogen surrounding gas and plasma assistance on nitrogen incorporation in aC: N films by femtosecond pulsed laser deposition. *Applied Surface Science*. **2016**, 374, pp.104-111.

[194] NEUVILLE, S. Quantum electronic mechanisms of atomic rearrangements during growth of hard carbon films. *Surface and Coatings Technology*. **2011**, 206(4), pp.703-726.

[195] NAKAZAWA, H., OSOZAWA, R., MOHNAI, Y. and NARA, Y. Synthesis of boron/nitrogen-incorporated diamond-like carbon films by pulsed laser deposition using nitrogen gas and a boron-containing graphite target. *Japanese Journal of Applied Physics*. **2017**, 56(10), p.105501.

[196] AL-RIYAMI, S., GIMA, H., AKAMINE, H. and YOSHITAKE, T. Chemical bonding of nitrogenated ultrananocrystalline diamond films deposited on titanium substrates by pulsed laser deposition. *ECS Journal of Solid State Science and Technology*. **2013**, 2(11), p.M33.

[197] PÍSAŘÍK, P., JELÍNEK, M., REMSA, J., MIKŠOVSKÝ, J., ZEMEK, J., JUREK, K., KUBINOVÁ, Š., LUKEŠ, J. and ŠEPITKA, J. Antibacterial, mechanical and surface properties of Ag-DLC films prepared by dual PLD for medical applications. *Materials Science and Engineering: C*. **2017**, *77*, pp.955-962.

[198] BUCHEGGER, S., VOGEL, C., HERRMANN, R., STRITZKER, B., WIXFORTH, A. and WESTERHAUSEN, C. Antibacterial metal ion release from diamond-like carbon modified

surfaces for novel multifunctional implant materials. *Journal of Materials Research*. **2016**, 31(17), pp.2571-2577.

[199] GUTENSOHN, K., BEYTHIEN, C., BAU, J., FENNER, T., GREWE, P., KOESTER, R., PADMANABAN, K. and KUEHNL, P. In Vitro Analyses of Diamond-like Carbon Coated Stents: Reduction of Metal Ion Release, Platelet Activation, and Thrombogenicity. *Thrombosis Research*. **2000**, 99(6), pp. 577-585.

[200] BOCIAGA, D., KOMOROWSKI, P., BATORY, D., SZYMANSKI, W., OLEJNIK, A., JASTRZEBSKI, K. and JAKUBOWSKI, W. Silver-doped nanocomposite carbon coatings (Ag-DLC) for biomedical applications–physiochemical and biological evaluation. *Applied Surface Science*. **2015**, *355*, pp.388-397.

[201] BOSETTI, M., MASSÈ, A., TOBIN, E. and CANNAS, M. Silver coated materials for external fixation devices: in vitro biocompatibility and genotoxicity. *Biomaterials*. **2002**, 23(3):887-892.

[202] KWOK, S. C. H., ZHANG, W., WAN, G. J., MCKENZIE, D. R., BILEK, M. M. M. and CHU, P. K. Hemocompatibility and anti-bacterial properties of silver doped diamond-like carbon prepared by pulsed filtered cathodic vacuum arc deposition. *Diamond and Related Materials*. **2007**, *16*(4-7), pp.1353-1360.

[203] CHEKAN, N. M., BELIAUSKI, N. M., AKULICH, V. V., POZDNIAK, L. V., SERGEEVA, E. K., CHERNOV, A. N., KAZBANOV, V. V. and KULCHITSKY, V. A. Biological activity of silver-doped DLC films. *Diamond and Related Materials*. **2009**, 18(5-8), pp.1006-1009.

[204] ZIA, A. W., ANESTOPOULOS, I., PANAGIOTIDIS, M. I., BOWEN, L. and BIRKETT, M. Biomechanical Characteristics of Silver Enriched Diamond-like Carbon Coatings for Medical Applications. *Journal of Alloys and Compounds*. **2023**, p.170473.

[205] LAN, W. C., OU, S. F., LIN, M. H., OU, K. L. and TSAI, M. Y. Development of silver-containing diamond-like carbon for biomedical applications. Part I: Microstructure characteristics, mechanical properties and antibacterial mechanisms. *Ceramics International*. **2013**, 39(4), pp.4099-4104.

[206] HATADA, R., FLEGE, S., BOBRICH, A., ENSINGER, W., DIETZ, C., BABA, K., SAWASE, T., WATAMOTO, T. and MATSUTANI, T. Preparation of Ag-containing diamond-like carbon films on the interior surface of tubes by a combined method of plasma source ion implantation and DC sputtering. *Applied surface science*. **2014**, *310*, pp.257-261.

[207] ZHANG, H. S., ENDRINO, J. L. and ANDERS, A. Comparative surface and nano-tribological characteristics of nanocomposite diamond-like carbon thin films doped by silver. *Applied Surface Science*. **2008**, 255(5), pp.2551-2556.

[208] AHMED, S. F., MOON, M. W. and LEE, K. R. Effect of silver doping on optical property of diamond like carbon films. *Thin Solid Films*. **2009**, 517(14), pp.4035-4038.

[209] HAUERT, R. and MÜLLER, U. An overview on tailored tribological and biological behavior of diamond-like carbon. *Diamond and Related Materials*. **2003**, 12(2), pp.171-177.

[210] KIM, J. H., SHIN, J. H., SHIN, D. H., MOON, M. W., PARK, K., KIM, T. H., SHIN, K. M., WON, Y. H., HAN, D. K. and LEE, K. R. Comparison of diamond-like carbon-coated nitinol stents with or without polyethylene glycol grafting and uncoated nitinol stents in a canine iliac artery model. *The British Journal of Radiology*. **2011**, 84(999), pp.210-215.

[211] ANDO, K., ISHII, K., TADA, E., KATAOKA, K., HIROHATA, A., GOTO, K., KOBAYASHI, K., TSUTSUI, H., NAKAHAMA, M., NAKASHIMA, H. and UCHIKAWA, S. Prospective multi-center registry to evaluate efficacy and safety of the newly developed diamond-like carbon-coated cobalt–chromium coronary stent system. *Cardiovascular intervention and therapeutics*. **2017**, 32, pp.225-232.

[212] DAMASCENO, J. C., CAMARGO JR, S. S., FREIRE JR, F. L., CARIUS, R. Deposition of Si-DLC films with high hardness, low stress and high deposition rates. *Surface and Coatings Technology*. **2000**, 133-134, pp.247-252.

[213] SOUM-GLAUDE, A., RAMBAUD, G., GRILLO, S. E. and THOMAS, L. Investigation of the tribological behavior and its relationship to the microstructure and mechanical properties of a-SiC: H films elaborated by low frequency plasma assisted chemical vapor deposition. *Thin Solid Films*. **2010**, *519*(4), pp.1266-1271.

[214] KIM, H. G., AHN, S. H., KIM, J. G., PARK, S. J. and LEE, K. R. Effect of Si-incorporation on wear-corrosion properties of diamond-like carbon films. *Thin Solid Films*. **2005**, 482(1-2), pp. 299-304.

[215] OGWU, A. A., OKPALUGO, T. I., ALI, N., MAGUIRE, P. D. and MCLAUGHLIN, J. A. Endothelial cell growth on silicon modified hydrogenated amorphous carbon thin films. *Journal of biomedical materials research. Part B, Applied biomaterials.* **2008**, 85(1), pp.105-113.

[216] OKPALUGO, T. I., MURPHY, H., OGWU, A. A., ABBAS, G., RAY, S. C., MAGUIRE, P. D., MCLAUGHLIN, J. and MCCULLOUGH, R. W. Human microvascular endothelial cellular interaction with atomic N-doped DLC compared with Si-doped DLC thin films. *Journal of biomedical materials research. Part B, Applied biomaterials.* **2006**, 78, pp.222-229.

[217] OKPALUGO, T. I., MCKENNA, E., MAGEE, A. C., MCLAUGHLIN, J. and BROWN, N. M. The MTT assays of bovine retinal pericytes and human microvascular endothelial cells on DLC and SiDLC-coated TCPS. *Journal of biomedical materials research. Part A.* **2004**, 71, pp.201-208.

[218] THORWARTH, G., SALDAMLI, B., SCHWARZ, F., JÜRGENS, P., LEIGGENER, C., SADER, R., HAEBERLEN, M., ASSMANN, W. and STRITZKER, B. Biocompatibility of

Doped Diamond-Like Carbon Coatings for Medical Implants. *Plasma Processes and Polymers*. **2007**, *4*(1), pp.364-368.

[219] ZHOU, X., ZHANG, N., MANKOCI, S. and SAHAI, N. Silicates in orthopedics and bone tissue engineering materials. *Journal of Biomedical Materials Research Part A*. **2017**, 105(7), pp.2090-2102.

[220] EISINGER, J. and CLAIRET, D. Effects of silicon, fluoride, etidronate and magnesium on bone mineral density: a retrospective study. *International Society for the Development of Research on Magnesium*. **1993**, 6(3), pp.247-249.

[221] ONG, S. E., ZHANG, S., DU, H., TOO, H. C. and AUNG, K. N. Influence of silicon concentration on the haemocompatibility of amorphous carbon. *Biomaterials*. **2007**, *28*(28), pp.4033-4038.

[222] OKPALUGO, T. I., OGWU, A. A., MAGUIRE, P. D., MCLAUGHLIN, J. A. D. Platelet adhesion on silicon modified hydrogenated amorphous carbon films. *Biomaterials*. **2004**, 25(2), pp.239-245.

[223] OKPALUGO, T. I., OGWU, A. A., MAGUIRE, P. D., MCLAUGHLIN, J. A. D. and HIRST, D. G. In-vitro blood compatibility of a-C:H:Si and a-C:H thin films. *Diamond and Related Materials*. **2004**, 13, pp.1088-1092.

[224] NAKAZAWA, H., OSOZAWA, R., OKUZAKI, T., SATO, N., SUEMITSU, M. and ABE, T. Effects of hydrogen on the properties of Si-incorporated diamond-like carbon films prepared by pulsed laser deposition. *Diamond and related materials*. **2011**, 20(4), pp.485-491.